

Interference effects in medium-induced gluon radiation

J. Casalderrey-Solana,^a E. Iancu,^{a,b}

^a*CERN, Theory Division, CH-1211 Geneva, Switzerland*

^b*Institut de Physique Théorique, CEA Saclay, F-91191 Gif-sur-Yvette, France*

E-mail: jorge.casalderrey@cern.ch, edmond.iancu@cea.fr

ABSTRACT: As a step towards understanding the in-medium evolution of a hard jet, we consider the interference pattern for the medium-induced gluon radiation produced by a color singlet quark-antiquark antenna embedded in a QCD medium with size L . We focus on the typical kinematics for medium-induced gluon radiation in the BDMPS-Z regime, that is, short formation times $\tau_f \ll L$ and relatively large emission angles $\theta \gg \theta_c \equiv 2/\sqrt{\hat{q}L^3}$, with \hat{q} the ‘jet quenching’ parameter. We demonstrate that, for a dipole opening angle $\theta_{q\bar{q}}$ larger than θ_c , the interference between the medium-induced gluon emissions by the quark and the antiquark is parametrically suppressed with respect to the corresponding direct emissions. Physically, this is so since the direct emissions can be delocalized anywhere throughout the medium and thus yield contributions proportional to L . On the contrary, the interference occurs only between gluons emitted at very early times, within the characteristic time scales for quantum and color coherence between the two emitters, which in this regime are much smaller than L . This implies that, for $\theta_{q\bar{q}} \gg \theta_c$, the medium-induced radiation by the dipole is simply the sum of the two BDMPS-Z spectra individually produced by the quark and the antiquark, without coherence effects like angular ordering. For $\theta_{q\bar{q}} \ll \theta_c$, the medium-induced radiation by the dipole vanishes.

Contents

1. Introduction	1
2. Physical discussion and summary	4
2.1 A primer on BDMPS–Z physics	4
2.2 Qualitative discussion of interference	8
3. General set–up and formalism	14
3.1 The amplitude for gluon emission	15
3.2 The ‘out–out’ terms as a warm up	20
4. Medium–induced gluon radiation: direct emission	23
5. Medium–induced gluon radiation: interference terms	30
6. Discussion and outlook	36
A. Momentum space analysis of the gluon spectrum	40
A.1 The gluon spectrum at the time of formation	41
A.2 The final gluon spectrum	42
A.3 Direct emission: the BDMPS–Z spectrum	44
A.4 The interference terms for relatively large dipoles: $\theta_f \lesssim \theta_{q\bar{q}} \lesssim \theta_s$.	44
A.5 The interference terms for relatively small dipoles: $\theta_c \ll \theta_{q\bar{q}} \ll \theta_f$.	45

1. Introduction

The phenomenon of *jet quenching* globally denotes the modifications in the properties of a jet which occur when the jet propagates through the dense QCD matter created in the intermediate stages of an ultrarelativistic heavy ion collision. One of the most striking effects of this kind is the large di–jet asymmetry observed in Pb+Pb collisions at the LHC, as reported by the ATLAS [1] and CMS [2] collaborations (see also [3] for related results at RHIC). These data imply that, as a consequence of the interactions between the jet and the medium, the jet energy is transported to larger angles and redistributed into softer fragments as compared to the p+p baseline. Understanding this phenomenon of strong jet broadening and also the strong suppression of particle production at high p_T in nucleus–nucleus collisions as compared to p+p, as observed at RHIC [4, 5, 6, 7] and the LHC [8], is essential for using jet probes as a diagnosis tool of hot and dense QCD matter.

From a microscopic point of view, the dominant mechanism for jet quenching at weak coupling and high energy is radiative energy loss associated with medium–induced gluon radiation [9, 10, 11, 12, 13, 14, 15, 16, 17] (see also the review papers [18, 19] for more references). If the

medium is sufficiently dense, both the parton that initiates the jet and its descendants undergo multiple scattering leading to additional radiation which is described by the BDMPS–Z (from Baier, Dokshitzer, Mueller, Peigné, Schiff, and Zakharov) formalism. While this mechanism for jet quenching has been quite successful in describing the suppression of single particle spectra observed at RHIC (see, for example [20, 21]), it has been realized for long that the respective data refer to inclusive measurements which are quite limited in constraining the underlying dynamics. By contrast, the differential jet measurements that are performed at the LHC provide more detailed informations, in particular, on the spectrum of the medium–induced radiation which could help us to better pinpoint the physical mechanisms at work.

At this point, one should stress that the BDMPS–Z mechanism predicts that gluons are emitted at relatively large angles — the softer the gluon, the larger its emission angle — and thus it has the potential to explain the di–jet asymmetry measured at the LHC (see the recent publications [22, 23, 24, 25] for related studies). However, from the experience with jet evolution in the vacuum, one knows that large angle radiation can be prohibited by coherence effects leading to *angular ordering*: within the partonic cascade produced via jet fragmentation in the vacuum, the emission angles are bound to decrease from one emission to the next one. So far very little is known about the corresponding property for the medium–induced gluon radiation. The only analyses in that sense so far [26, 27] are either restricted to the single–scattering approximation [26] or concerned with a different mechanism for medium–induced radiation [27], which applies to relatively soft and collinear emissions which are less effective in broadening the transverse energy distribution of a jet.

It is therefore crucial to clarify whether interference effects can frustrate medium–induced radiation at large angles, in the interesting regime where the medium is relatively opaque and the multiple scattering is important. This is the main objective in this paper. To that aim, we shall study the interference between the medium–induced gluon emissions by two sources immersed into the medium: a quark (q) and an antiquark (\bar{q}). More precisely, we shall address the problem of the in–medium ‘dipole antenna pattern’, that is, the radiation produced by a $q\bar{q}$ pair in a color singlet state (a ‘color dipole’) where the two particles separate from each other at constant velocities which make a relative angle $\theta_{q\bar{q}}$ — the dipole opening angle. This ‘dipole antenna’ is a familiar set–up for studies of interference and angular ordering for radiation in the vacuum [28, 29] and has been generalized in Refs. [26, 27] to corresponding studies in a medium. As usual in the related literature, we shall work in the ‘multiple soft scattering approximation’ which assumes that successive scattering centers are independent from each other. Formally, the results of Ref. [26] can be recovered from this formalism as the lowest order term in the ‘opacity expansion’, that is, the perturbative expansion of the medium effects. But this is only formal, since the effects of multiple scattering are non–perturbative and the final results cannot be expanded out anymore¹. In that sense, we expect our conclusions to differ from those in Ref. [26] at *qualitative* level, and not only quantitatively.

The main conclusion which emerges from our analysis is that the interference effects for medium–induced gluon radiation are parametrically small and hence irrelevant for all values of the dipole angle $\theta_{q\bar{q}}$ except for very small values $\theta_{q\bar{q}} \lesssim \theta_c$, where direct emissions and interference

¹This is similar to the failure of the twist expansion for high–energy scattering in the vicinity of the unitarity limit, or in the gluon saturation region.

terms become comparable with each other, and even cancel each other when $\theta_{q\bar{q}} \ll \theta_c$.

In order to explain this conclusion and in particular the special angle θ_c , we need to first recall some basic features of the BDMPDS–Z mechanism (see Sect. 2 for a physical discussion). The corresponding phase–space is characterized by two limiting values, a maximal frequency ω_c and a minimum angle θ_c , which are expressed in terms of the medium properties as $\omega_c = \hat{q}L^2/2$ and $\theta_c = 2/\sqrt{\hat{q}L^3}$. (\hat{q} is the jet quenching parameter and L is the longitudinal extent of the slice of the medium which is crossed by the dipole.) The energy loss by the leading particle is dominated by the emission of relative hard gluons with $\omega \simeq \omega_c$, but such gluons make a small angle $\theta \simeq \theta_c$ with respect to their source and thus are not effective in broadening the jet energy distribution in the transverse plane. Rather, the dominant transverse broadening comes from softer gluons with $\omega \ll \omega_c$, which are emitted at relatively large angles $\theta \gtrsim \theta_f(\omega) \gg \theta_c$. Here, $\theta_f(\omega)$ is the minimal emission angle for a gluon with frequency ω (the ‘formation angle’) and increases when decreasing ω below ω_c .

An important property of these soft gluons, which is favorable too for the physics of jet broadening, is the fact that they are *promptly* emitted: the corresponding formation time is much smaller than the medium length L . Hence, such gluons can be emitted at any point inside the medium. Accordingly, the longitudinal phase–space for *direct* emissions by the quark or the antiquark is proportional to L . By contrast, the *interference* between the two partonic sources occurs only for the gluons emitted at sufficiently early times $t < \tau_{min}$, when the quark and the antiquark are still close enough to each other to ensure *color* and *quantum coherence*. The precise mechanism which determines τ_{min} depends upon the value of the dipole angle $\theta_{q\bar{q}}$: (i) when $\theta_c \ll \theta_{q\bar{q}} \ll \theta_f(\omega)$, the interference is limited by the *color decoherence* of the $q\bar{q}$ pair (the two sources suffer different color precessions in the medium); (ii) when $\theta_{q\bar{q}} \gtrsim \theta_f(\omega)$, τ_{min} is rather determined by the condition of *quantum coherence* (the radiated gluon must overlap with both sources). But in both cases, *i.e.* so long as $\theta_{q\bar{q}} \gg \theta_c$, this upper limit τ_{min} is much smaller than L , meaning that the phase–space for interference, which is proportional to τ_{min} , is parametrically suppressed relative to that for direct emissions. Then the interference effects are negligible. On the other hand, when $\theta_{q\bar{q}} \lesssim \theta_c$, τ_{min} becomes as large as L , so the interference is not suppressed anymore. But then the total medium–induced radiation vanishes, since a gluon emitted at an angle $\theta \gtrsim \theta_f(\omega) \gg \theta_c$ ‘sees’ the total color charge of the $q\bar{q}$ pair, which is zero.

To summarize, the medium–induced radiation by the dipole is non–zero only when $\theta_{q\bar{q}} \gg \theta_c$ and in that case it is simply the sum of the two BDMPS–Z spectra separately produced by the two emitters, without any coherence effect like angular ordering. In order to substantiate this conclusion and the above physical picture, we shall explicitly estimate the contribution of the interference effects to the spectrum of the medium–induced radiation by the dipole and compare the result with the corresponding contribution due to direct emissions. Our main results in that sense, namely Eq. (5.14) for the contribution of the interference terms and Eq. (4.21) for that of the direct emissions, are confirmed by two different calculations (one exposed in the main text, the other one in the Appendix), which involve approximation schemes with different degrees of rigor, but which agree with each other to parametric accuracy.

Our paper is organized as follows: In Sect. 2 we present a qualitative discussion of the medium–induced radiation, including the BDMPS–Z mechanism (for completeness and pedagogy), but focusing on our original results on interferences. Our purpose there is to motivate

our conclusions via physical considerations, which hopefully will provide the guidelines for the subsequent, more formal, developments. In Sect. 3, we give a streamlined presentation of the BDMPS–Z formalism adapted to the problem at hand and also make contact with the analysis in Ref. [27]. Sects. 4 and 5 are the main sections of this paper. They present detailed calculations of the medium–induced contributions to direct emissions (Sect. 4) and to the interference terms (Sect. 5). To keep the presentation as fluent as possible, in these sections we resort on analytic approximations which are correct at parametric level. (More refined versions of these calculations are deferred to Appendix A.) This allows us to provide an explicit expression for the BDMPS–Z spectrum (consistent with the respective results in the literature) and to deduce an equally explicit result for the interference contribution to the spectrum. Finally, in Sect. 6 we discuss the implications of our results for the in–medium evolution of a hard jet and we mention some open problems.

Note added

When this work was already finished, a preprint appeared, Ref. [30], in which the general formula for the interference contribution to the medium–induced radiation by the dipole (our Eq. (5.2)) was also derived. However, the physical consequences of this formula were not explicitly worked out. In particular Ref. [30] did not identify the physical mechanism responsible for the suppression of the in–medium interference terms, which is the reduction in the corresponding longitudinal phase–space. The conclusions drawn there by inspection of the general formula turned out to be incorrect in some cases. In the mean time, such issues have been clarified via private communications.

2. Physical discussion and summary

We start our presentation with a section which summarizes, at a qualitative level, the physical picture and the main conclusions that we shall eventually reach through our analysis. This strategy of presentation is motivated by the fact that the physical problems that we shall address are both complex and subtle, as they involve several (time and momentum) scales and also non–perturbative phenomena (like high density effects). The theoretical treatment of these phenomena will therefore be quite involved and lengthy. Notwithstanding, the ultimate physical picture which will emerge from our calculations is quite simple and can be transparently structured in terms of a hierarchy of (time and angular) scales, which for the benefit of the reader are summarized in Table 1. So we feel that the reading of the paper will gain in clarity if the relevant scales are *a priori* identified, via physical considerations, and if the final conclusions are exposed on the basis on these scales alone. This will motivate the subsequent, more formal, manipulations and hopefully provide the guidelines for the approximations to come. The discussion in this section is intended to be self–contained (provided, of course, the reader will be ready to accept some arguments to be rigorously demonstrated later) and could be read as a summary of our present work, independently of the subsequent, more formal developments.

2.1 A primer on BDMPS–Z physics

The propagation of a high energy parton through a dense QCD medium leads to energy loss and transverse momentum broadening via *medium–induced radiation*, that is, the emission of gluons

stimulated by the interactions between the quark, or the radiated gluon, and the medium. The radiation process requires a characteristic *formation time* which can be understood as the time for the (virtual) gluon to separate enough from its parent quark for the quantum (in particular, color) coherence between the two quanta to be lost. This formation time τ_q can be estimated from the condition that the transverse separation $b_\perp = \tau_q v_\perp$ between the quark and the gluon at the formation time be of the order of the gluon transverse wavelength $\lambda_\perp = 1/k_\perp$. Here ‘transverse’ refers to the direction orthogonal to the trajectory of the quark, k_\perp is the gluon transverse momentum and $v_\perp = k_\perp/\omega$ is its transverse velocity. We have also introduced the gluon energy ω , assumed to be large compared to k_\perp . Accordingly, the gluon emission angle is small, $\theta_q \simeq k_\perp/\omega \ll 1$. The previous discussion implies²

$$\tau_q \frac{k_\perp}{\omega} \simeq \frac{2}{k_\perp} \implies \tau_q \simeq \frac{2\omega}{k_\perp^2} \simeq \frac{2}{\omega\theta_q^2}. \quad (2.1)$$

The above argument is completely general: it holds for gluon emissions in either the medium or the vacuum. What is different, however, is the typical value of k_\perp in the two cases.

For emissions in the vacuum, k_\perp is *a priori* arbitrary. However, the associated, bremsstrahlung, spectrum

$$\omega \frac{dN^{\text{vac}}}{d\omega dk_\perp^2} \simeq \frac{\alpha_s C_F}{k_\perp^2} \simeq \alpha_s C_F \theta_q^2 \tau_q^2, \quad (2.2)$$

is such that large values of k_\perp are strongly suppressed, so most of the radiation is quasi-collinear with its source ($\theta_q \rightarrow 0$). The second equality in Eq. (2.2), which is clearly true in view of Eq. (2.1), has a simple physical interpretation. After the quark is created at $t_0 = 0$, a gluon with energy ω and transverse momentum k_\perp is emitted by a time $t \sim \tau_q$ and not much later. Then the integral over time which enters the calculation of the emission amplitude (see Sect. 3.1 below) yields a factor τ_q . Correspondingly, there will be a factor τ_q^2 in the emission probability which represents the temporal (or longitudinal) phase-space for gluon emissions in the vacuum. The factor θ_q^2 is the square of the transverse velocity $v_\perp \simeq \theta_q$ of the emitted gluon, which is the emission vertex in a vectorial, gauge, theory.

Within a medium, on the other hand, the gluon can acquire an additional transverse momentum via scattering off the medium constituents, both during the formation time and after (see the graphical representation in Fig. 1). If the medium is sufficiently dense, the momentum acquired in this way can be large and then the gluon spectrum is shifted towards a non-zero central value. At weak coupling, one can assume that successive collisions in the medium proceed independently from each other, even when the medium is dense: the gluon mean free path ℓ scales like $1/\alpha_s$ and for sufficiently small $\alpha_s = g^2/(4\pi)$ it becomes much larger than the screening length $\mu_D^{-1} \propto 1/g$ for charge correlations in the medium (μ_D is the Debye mass). The gluon receives random kicks from the medium constituents, with each kick transferring a momentum squared $\sim \mu_D^2$, so its *average* transverse momentum squared grows at a rate

$$\frac{d\langle k_\perp^2 \rangle}{dt} \simeq \frac{\mu_D^2}{\ell} \equiv \hat{q}. \quad (2.3)$$

²The factor of 2 in Eq. (2.1) is conventional; this result is to be seen as a parametric estimate, valid within the limits of the uncertainty principle.

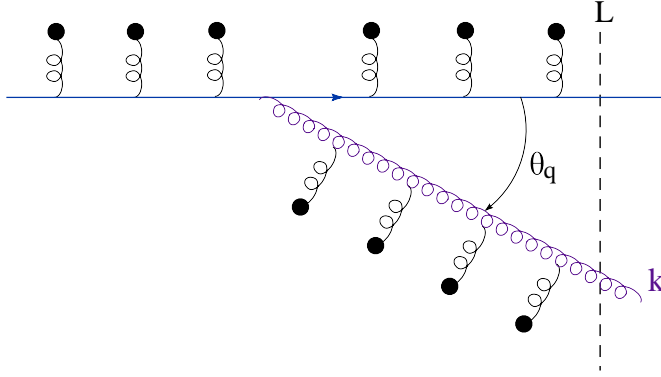


Figure 1: The standard representation of the Feynman graph for medium-induced gluon radiation: both the quark and the emitted gluon undergo multiple scattering off the medium constituents.

The quantity \hat{q} is a local transport coefficient known as the *jet quenching parameter*.

Returning to the process of gluon emission, we see that the gluon can be set free by its interactions with the medium, which then determine the *in-medium formation time* τ_f . Specifically, within a time τ_f , the gluon acquires a transverse momentum squared $k_f^2 \simeq \hat{q}\tau_f$ with τ_f related to k_f^2 as shown in Eq. (2.1). We thus deduce

$$k_f^2 \simeq (2\omega\hat{q})^{1/2} \quad \text{and} \quad \tau_f \simeq \sqrt{\frac{2\omega}{\hat{q}}}. \quad (2.4)$$

We see that the medium rescattering controls the formation time τ_f , the gluon average transverse momentum at the time of formation, k_f , and hence also the *formation angle* $\theta_f \simeq k_f/\omega$. In order for the gluon to be formed in the medium, one needs, clearly, $\tau_f \leq L$, with L the longitudinal extent of the slice of the medium which is crossed by the quark. Hence, the maximal possible value for k_f , known as the *saturation momentum* Q_s , is given by $Q_s^2 = \hat{q}L$ and is achieved for a gluon with a frequency ω_c such that $\tau_f(\omega_c) = L$. These relations imply

$$\omega_c = \frac{1}{2}\hat{q}L^2, \quad Q_s^2 = \hat{q}L, \quad \theta_c = \frac{Q_s}{\omega_c} = \frac{2}{Q_s L} = \frac{2}{\sqrt{\hat{q}L^3}}. \quad (2.5)$$

θ_c is the formation angle for a gluon with frequency ω_c and is the minimal angle in the problem: gluons with larger frequencies $\omega > \omega_c$ and smaller angles $\theta_q < \theta_c$ cannot be emitted via this mechanism. The medium is *dense* provided the transverse momentum k_f acquired by the gluon via multiple scattering during the process of formation is much larger than the Debye mass μ_D . In view of Eq. (2.3), this requires the in-medium formation time τ_f to be substantially larger than the mean free path ℓ , and hence even more so as compared to the Debye length: $\tau_f \gg \ell \gg \mu_D^{-1}$. Since, moreover, $Q_s > k_f$ and $L > \tau_f$, these relations imply that the limiting angle $\theta_c \sim 1/(Q_s L)$ is truly small: $\theta_c \ll 1$. (Some typical values for heavy ion collisions at RHIC and the LHC are $L = 6$ fm and $\hat{q} = 2 \div 10$ GeV²/fm, yielding $\theta_c = 0.005 \div 0.01$.)

More generally, for a given energy $\omega < \omega_c$, the quantities k_f and θ_f introduced above — the average transverse momentum and emission angle *at the formation time* — represent lower limits on the respective kinematical variables in the BDMPS-Z spectrum. For what follows, it is useful to express the *quasi-local* quantities k_f and θ_f , which are controlled by the physics at

the scale τ_f , in terms of the *global* (L -dependent) quantities in Eq. (2.5), which represent their absolute limits attained when $\tau_f = L$:

$$\tau_f = L\sqrt{\frac{\omega}{\omega_c}}, \quad k_f = Q_s \left(\frac{\omega}{\omega_c}\right)^{1/4}, \quad \theta_f \equiv \frac{k_f}{\omega} = \theta_c \left(\frac{\omega_c}{\omega}\right)^{3/4}. \quad (2.6)$$

These formulæ make clear that the *relatively soft* gluons with $\omega \ll \omega_c$ are emitted *very fast* ($\tau_f \ll L$) and at *relatively large angles* ($\theta_f \gg \theta_c$). Such gluons are very efficient in broadening the jet energy in the transverse plane.

While the quark propagates through the medium it receives kicks from the medium constituents and it can radiate after any of those kicks. The typical distance ℓ between two consecutive kicks is generally much shorter than the formation time of the gluon τ_f ; accordingly, a large number of scattering centers $N_{coh} \simeq \tau_f/\ell \gg 1$ will coherently act as a single source of radiation. This subset of N_{coh} constituents can be located anywhere inside the medium, meaning that the time t_1 at which a particular emission is initiated is delocalized within the interval $0 \leq t_1 \leq L$. Thus, unlike vacuum emissions which start right away after a hard scattering, the medium-induced emissions can be initiated at any point inside the medium. Accordingly, the longitudinal phase-space for medium-induced gluon radiation is $(L - \tau_f)\tau_f \sim L\tau_f$, which for $\omega \ll \omega_c$ is *parametrically larger* than the corresponding bremsstrahlung phase-space τ_q^2 (for the same kinematics). We shall later derive the gluon spectrum *at the formation time* and thus find a Gaussian centered at k_f :

$$\omega \frac{dN}{d\omega dk_{\perp}^2} \Big|_{\text{form}} \propto \alpha_s C_F \theta_q^2 \tau_f L \exp\left\{-\frac{k_{\perp}^2}{k_f^2}\right\}. \quad (2.7)$$

The prefactor in this expression is similar to that in Eq. (2.2): the only difference refers to the replacement $\tau_q^2 \rightarrow \tau_f L$ for the longitudinal phase-space. Since $\theta_q \propto k_{\perp}$, it is clear that this spectrum is strongly peaked at $k_{\perp} = k_f$. Hence, for parametric estimates, one can replace $\theta_q \rightarrow \theta_f$ in the prefactor. For $k_{\perp} \sim k_f$ and $\omega \ll \omega_c$, one has $\tau_q \sim \tau_f \ll L$, hence Eq. (2.7) is indeed enhanced w.r.t. the vacuum spectrum (2.2), by the large factor $L/\tau_f \gg 1$. This factor counts the number of times that a medium-induced gluon can be formed inside the medium.

Eq. (2.7) is not yet the final BDMPS-Z spectrum since after being formed, the gluon will still propagate inside the medium over a distance $L - \tau_f - t_1$, with $0 < t_1 < L - \tau_f$, and thus acquire an additional momentum broadening $\Delta k_{\perp}^2 \simeq \hat{q}(L - \tau_f - t_1)$. Accordingly, its final momentum $k_{\perp}^2 = k_f^2 + \Delta k_{\perp}^2$ can take any value from $k_f^2 = \hat{q}\tau_f$ to $Q_s^2 = \hat{q}L$. This results in the following kinematics domain for the final gluon, as measured by a detector:

$$\hat{q}^{1/3} \lesssim \omega \lesssim \omega_c, \quad k_f \lesssim k_{\perp} \lesssim Q_s. \quad (2.8)$$

The lower limit $\hat{q}^{1/3}$ on ω comes from the condition that $\omega > k_{\perp} > k_f$. Within this range in k_{\perp} , the BDMPS-Z distribution is roughly flat (see Eq. (4.22) below).

In discussing interference phenomena in what follows, it will be more convenient to use angular variables instead of transverse momenta. Using Eq. (2.8), one immediately finds the following range for the *final* gluon angle $\theta_q \simeq k_{\perp}/\omega$:

$$\theta_f \equiv \theta_c \left(\frac{\omega_c}{\omega}\right)^{3/4} \lesssim \theta_q \lesssim \theta_s \equiv \theta_c \frac{\omega_c}{\omega}. \quad (2.9)$$

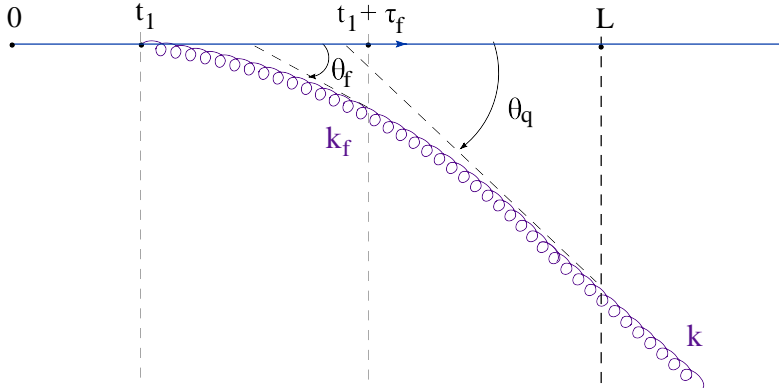


Figure 2: A cartoon illustrating the space–time picture of a medium–induced gluon radiation. The gluon formation is initiated at time t_1 and terminated at time $t_1 + \tau_f$. The gluon leaves the medium with its final momentum \mathbf{k} at time L . The interactions with the medium are not explicitly shown.

Clearly, θ_s (the ‘saturation angle’) is the same as $\theta_s = Q_s/\omega$. For $\omega \ll \omega_c$, the final angle θ_q is much larger than θ_c — at least as large as θ_f . The space–time picture and the main scales for medium–induced radiation are illustrated in Fig. 2.

2.2 Qualitative discussion of interference

To study interference effects, we shall replace the quark probe considered in the previous subsection with a color dipole, that is a quark (q) and antiquark (\bar{q}) in a color singlet state which separate from each other at constant velocities which make a relative angle $\theta_{q\bar{q}}$ — the dipole opening angle. The quark and the antiquark are massless, so they propagate at the speed of light. The dipole is created at time $t_0 = 0$ and for later times its transverse size grows like $r_\perp(t) \simeq \theta_{q\bar{q}} t$. (We assume the dipole angle to be relatively small, $\theta_{q\bar{q}} \ll 1$. For the case of medium–induced emission, this angle should be correlated with the respective emission angles, as we shall later discuss.) By ‘transverse’ we here mean the direction perpendicular to the common direction of motion of the quark and the antiquark (the ‘longitudinal axis’), as defined by the trajectory of their center of mass. Interference occurs if the transverse wavelength of the gluon which is about to be emitted is large enough for the gluon to have an overlap with both sources. When this happens, the gluon ‘sees’ the overall color charge of the $q\bar{q}$ pair, which is zero, so it is not emitted anymore (destructive interference).

Let us first recall the respective argument in the case of the vacuum, where it is well known to lead to *angular ordering*. The distance between the quark and the antiquark at the time of emission is, roughly, $\theta_{q\bar{q}} \tau_q$ with $\tau_q = 2\omega/k_\perp^2$. (We assume the gluon to be emitted by the quark.) Interference occurs if this distance is smaller than the transverse wavelength $\lambda_\perp \simeq 1/k_\perp$ of the gluon. Using $k_\perp \simeq \omega\theta_q$, with θ_q the angle of emission, we deduce

$$\theta_{q\bar{q}} \frac{1}{\omega\theta_q^2} \lesssim \frac{1}{\omega\theta_q} \quad \Longrightarrow \quad \theta_q \gtrsim \theta_{q\bar{q}}. \quad (2.10)$$

That is, the interference is important only for gluon emissions at relatively large angles, outside of the dipole cone.

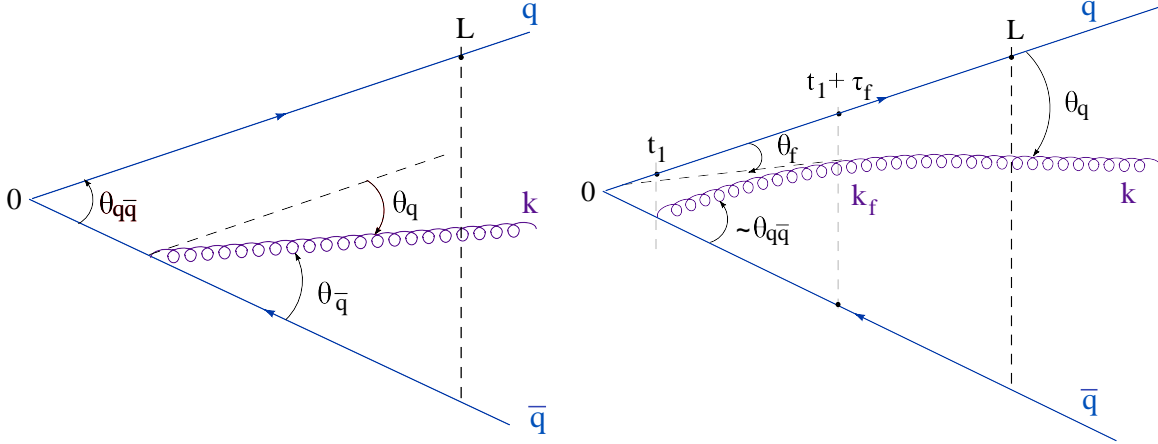


Figure 3: Gluon emission by the dipole. Left: the geometry of the final state. Right: The space–time picture of a typical emission contributing to interference in the case $\theta_{q\bar{q}} > \theta_f$. When the emission is initiated, at time $t_1 \sim \tau_{int}$ by the antiquark, the virtual gluon is co–moving with the quark. When the emission is completed, at time $t_1 + \tau_f$, the gluon makes an angle θ_f with the quark.

The interference effects can be also discussed at the level of the bremsstrahlung spectrum produced by the dipole. This is given by the following generalization of Eq. (2.2)

$$\omega \frac{dN_{\text{dip}}^{\text{vac}}}{d^3\mathbf{k}} \simeq \alpha_s C_F (\theta_q \tau_q - \theta_{\bar{q}} \tau_{\bar{q}})^2, \quad (2.11)$$

with $k^\mu = (\omega, \mathbf{k})$ the 4–vector of the emitted gluon, $\tau_q \simeq 2/(\omega\theta_q^2)$ and $\tau_{\bar{q}} \simeq 2/(\omega\theta_{\bar{q}}^2)$. (Note that our sign conventions for the emission angles are such that $\theta_q < 0$ and $\theta_{\bar{q}} > 0$ for emissions inside the dipole and $\theta_q \theta_{\bar{q}} > 0$ for emissions outside the dipole; see also Fig. 3 left. With this convention, one has $\theta_{q\bar{q}} = \theta_{\bar{q}} - \theta_q > 0$. Also, when using an angle within a parametric estimate or an inequality, we always mean its absolute value.) By expanding the square in the r.h.s. one generates the *direct emission* terms, from the quark ($\theta_q^2 \tau_q^2$) and respectively the antiquark ($\theta_{\bar{q}}^2 \tau_{\bar{q}}^2$), together with the *interference term* $-2\theta_q \theta_{\bar{q}} \tau_q \tau_{\bar{q}}$, which has an overall minus sign because the two sources have opposite charges. Inside the dipole cone, where the two emission angles have opposite signs, the interference term is relatively unimportant: the radiation is strongly peaked around the direction of the quark ($\theta_q \approx 0$) or of the antiquark ($\theta_{\bar{q}} \approx 0$), where it is dominated by the respective direct emission. However for large emission angles $\theta_q, \theta_{\bar{q}} \gg \theta_{q\bar{q}}$ one has $\theta_q \simeq \theta_{\bar{q}}$ and $\tau_q \simeq \tau_{\bar{q}}$ and then the total radiation vanishes — the direct emissions are compensated by the interference term.

We now turn to the description of the medium–induced gluon radiation from an energetic $q\bar{q}$ dipole created in the medium. It is intuitively clear that, if the dipole angle is sufficiently large (larger than the maximal emission angle θ_s introduced in the previous subsection, cf. Eq. (2.9)), the radiation patterns produced by the quark and the antiquark via interactions in the medium have no overlap with each other and thus they are independent. The question we would like to address is what happens when the dipole opening angle is not that large. In that case, and in view of the experience with radiation in the vacuum, one may expect the dipole antenna pattern to be affected by interference effects between the emissions by the quark and the antiquark. However, as we shall now argue, this expectation is generally incorrect: for a sufficiently dense

medium and a dipole angle $\theta_{q\bar{q}}$ which is not very small (see below for the precise condition), only those gluons which are emitted very close to the $q\bar{q}$ vertex can be coherent with both emitters and thus lead to interference. Accordingly, the interference effects are parametrically suppressed as compared to the direct emissions from each of the quarks.

Our subsequent arguments will heavily rely on the three main properties of the medium-induced radiation (by a single source), as described in Section 2.1 and that we summarize here for further convenience:

1. The formation of a medium-induced gluon takes a time τ_f . When the gluon is formed it is emitted at a typical angle θ_f from the parent quark, that is, it carries a typical transverse momentum $k_f \simeq \omega\theta_f$.
2. After formation, multiple scattering leads to an additional broadening of the gluon spectrum. The final gluon distribution is concentrated within a typical angle $\theta_s > \theta_f$ around the parent parton.
3. As long as $\tau_f \ll L$, gluons are emitted all along the medium length L . As a consequence, the medium-induced gluon spectrum is proportional to L .

The concept of *coherence* will play an important role in the subsequent discussion of interference effects in the medium-induced gluon radiation. But as we shall see, several types of coherence come into the play and, moreover, some of them are not specific to the interference phenomena, but also occur for the direct emissions. Specifically, the process of in-medium gluon formation is by itself a phenomenon of *decoherence*: it proceeds via the gradual loss (due to interactions in the medium) of the coherence between the virtual gluon and the partonic sources which compose the dipole. This applies to all the emissions of the BDMPS-Z type — direct emissions and interferences. In addition, the interference phenomena require the two partonic sources (q and \bar{q}) to be *coherent* with each other during the gluon formation. In turn, this last requirement has *two* aspects: (i) *quantum* coherence, namely the emitted gluon needs to overlap with both sources, and (ii) *color* coherence, that is, the $q\bar{q}$ pair needs to preserve its original, overall, color charge — here, to remain in a color singlet state. Each of these coherence phenomena introduces a characteristic time (or length) scale, that we shall shortly describe.

(i) **Quantum coherence.** The emission process preserves the quantum coherence of the $q\bar{q}$ system so long as the virtual gluon overlaps with both sources in the course of formation. (After formation, the multiple scattering of the gluon in the medium can change the gluon momentum but it cannot affect the interference process since the gluon is already decorrelated from both partonic sources.) For that to be possible, the transverse resolution of the gluon at the time of formation, as measured by the respective transverse wavelength $\lambda_f = 1/k_f$, should be larger than the typical distance between the quark and the antiquark around that time. For emissions in the vacuum, this condition immediately leads to angular ordering, as discussed around Eq. (2.10). But for the medium-induced emissions, the situation is more subtle: during the gluon formation, the transverse size of the $q\bar{q}$ system increases from $r_{min} \simeq \theta_{q\bar{q}} t_1$ to $r_{max} \simeq \theta_{q\bar{q}} t_2$; here, t_1 is the time when the emission is initiated and can be delocalized anywhere within the medium, while $t_2 = t_1 + \tau_f$ is the time when the emission is completed. Then it is not *a priori* clear which one among these scales, r_{min} or r_{max} , should be compared to λ_f . Yet, our calculations, to be

detailed in Sect. 5 and in Appendix A, yield an unambiguous answer to this question: the $q\bar{q}$ size to be compared with λ_f is the *geometric average* of these two extreme scales. That is, the condition of quantum coherence amounts to $\sqrt{r_{min}r_{max}} \lesssim \lambda_f$, or

$$\sqrt{t_1(t_1 + \tau_f)} \lesssim \frac{\lambda_f}{\theta_{q\bar{q}}} \equiv \tau_\lambda. \quad (2.12)$$

Most likely, the appearance of the geometrical average in the l.h.s. reflects the fact that the gluon undergoes transverse diffusion during the formation process (see Sects. 4 and 5 below). The r.h.s. of Eq. (2.12) defines the *transverse resolution time* τ_λ , which is the scale controlling quantum coherence in the interference of the BDMPS–Z gluons. Using $\lambda_f = 1/k_f$ with k_f given by Eq. (2.4), it is easily to see that

$$\tau_\lambda = \frac{1}{\theta_{q\bar{q}}(\hat{q}\omega)^{1/4}} = \tau_f \frac{\theta_f}{\theta_{q\bar{q}}}, \quad (2.13)$$

where the second estimate follows since $k_f \simeq \omega\theta_f$ and $\tau_f \simeq 2/(\omega\theta_f^2)$.

Eq. (2.12) implies an upper limit on y^+ that we shall now explicitly work out. The second estimate in Eq. (2.13), which compares τ_λ to τ_f , makes clear that there are two limiting regimes, depending upon the ratio $\theta_{q\bar{q}}/\theta_f$:

(i. a) For relatively small dipole angles $\theta_{q\bar{q}} \ll \theta_f$, one has $\tau_\lambda \gg \tau_f$ and then Eq. (2.12) implies $y^+ \lesssim \tau_\lambda$. This upper limit is relatively large showing that, in this case, quantum coherence is relatively easy to ensure. This is natural: during the formation process, the BDMPS–Z spectra produced by the two emitters are confined to angles $\lesssim \theta_f$ around their respective sources. So, if the dipole angle is much smaller than θ_f , these two spectra have a strong overlap with each other and can interfere.

(i. b) For larger dipole angles $\theta_{q\bar{q}} \gg \theta_f$, one has $\tau_\lambda \ll \tau_f$ and therefore $t_1 \ll \tau_f$ as well. (Indeed, t_1 is strictly smaller than τ_λ , as obvious from Eq. (2.12).) Using this information, the condition (2.12) simplifies to

$$t_1 \lesssim \frac{\tau_\lambda^2}{\tau_f} \equiv \tau_{int}, \quad (2.14)$$

which introduces a new scale τ_{int} , the *interference time*. This scale can be rewritten as

$$\tau_{int} = \frac{2}{\omega\theta_{q\bar{q}}^2} = \tau_f \left(\frac{\theta_f}{\theta_{q\bar{q}}} \right)^2, \quad (2.15)$$

where the first expression is recognized as the *vacuum-like* formation time for a gluon emitted at an angle $\sim \theta_{q\bar{q}}$. This situation is reminiscent of the interference phenomena in the vacuum (cf. Eq. (2.10)): for the interference to be possible, the process must begin with the emission of a gluon at a relatively large angle, of order $\theta_{q\bar{q}}$, with respect to its parent quark. Of course, this gluon could then interfere with a similar, large-angle, emission by the other quark; if so, it would contribute to the interference piece of the bremsstrahlung spectrum in Eq. (2.11). Alternatively — and this is, of course, the situation that we are currently interested in —, it can interfere with a medium-induced emission by the other quark. Indeed, among the gluons emitted by one parton (say, the antiquark) at an angle $\gtrsim \theta_{q\bar{q}}$, there is a non-trivial fraction which are co-moving with

the *other* parton (the quark). These gluons overlap with the quark and are co-moving with it, so they cannot be distinguished from the typical gluons from the *quark* wavefunction. Accordingly, they will follow the formation process for in-medium radiation by the *quark* and eventually emerge (at time $t_1 + \tau_f$) at an angle θ_f w.r.t. the latter. This process, which is qualitatively illustrated in Fig. 3 right, will yield an interference contribution to the BDMPS-Z spectrum of the dipole, whose phase-space however is relatively small, since restricted by τ_{int} .

(ii) **Color coherence.** In addition to quantum coherence, the existence of interference effects between the two partonic emitters require the preservation of the color coherence between the quark and the antiquark. In the vacuum, the color state of the dipole is conserved until a gluon emission takes place and the interference pattern is governed solely by quantum coherence. In the medium, on the contrary, the interactions with the medium constituents change the color of each of the propagating parton (via ‘color rotation’). For a very energetic parton, this rotation amounts to multiplying the respective wavefunction by a $SU(N_c)$ matrix-valued phase — a Wilson line — which involves the random color field generated by the charged constituents of the medium evaluated along the trajectory of the particle.

For the $q\bar{q}$ pair we have two such Wilson lines which diverge from each other (since so do the quark and the antiquark) at constant angle $\theta_{q\bar{q}}$. The color coherence is measured by the 2-point correlation function of these Wilson lines, as obtained after averaging over the fluctuations of the background field. Within the ‘multiple soft scattering approximation’, this 2-point function can be computed to all orders in the medium effects. The results of these calculations, to be detailed in Sects. 3.2 and 5, show that the quark and the antiquark lose any trace of their original color correlation after the *decoherence time*

$$\tau_{coh} = \frac{2}{(\hat{q}\theta_{q\bar{q}}^2)^{1/3}} = \tau_f \left(\frac{\theta_f}{\theta_{q\bar{q}}} \right)^{2/3}. \quad (2.16)$$

Accordingly, this scale too acts as an upper limit on t_1 : there is no interference between the two partonic sources for the gluons whose emission is initiated at a time t_1 larger than τ_{coh} . It will be later useful to have a direct comparison between this scale τ_{coh} and the medium length L . This is obtained from Eq. (2.16) and Eq. (2.6) as

$$\tau_{coh} \simeq \left(\frac{\theta_c}{\theta_{q\bar{q}}} \right)^{2/3} L. \quad (2.17)$$

Quite remarkably, this estimate involves the limiting angle θ_c of the BDMPS-Z spectrum, although the present physical context is quite different: the scale τ_{coh} refers to the color coherence between the two emitters *independently* of their radiation.

From the previous discussion, we see that the analysis of interference effects in the medium-induced dipole radiation is a multi-scale problem. While the details of the in-medium dipole antenna pattern are expected to depend upon all these scales, the phase-space for interference is controlled by the *smallest* of them, $\tau_{min} = \min(\tau_\lambda, \tau_{int}, \tau_{coh})$. Indeed, the coherence of the $q\bar{q}$ dipole is only preserved at times which are simultaneously shorter than any of these scales. As a consequence, the interference contribution to the gluon spectrum (that is, the contribution of diagrams in which the gluon is emitted by the quark in the amplitude and by the antiquark in the complex conjugate amplitude, or *vice versa*), does not scale with the medium length, as the emission from each of the sources does, but with τ_{min} .

Remarkably, Eqs. (2.13), (2.15) and (2.16), which can be summarized as

$$\tau_f \sim \tau_{coh} \left(\frac{\theta_{q\bar{q}}}{\theta_f} \right)^{2/3} \sim \tau_\lambda \frac{\theta_{q\bar{q}}}{\theta_f} \sim \tau_{int} \left(\frac{\theta_{q\bar{q}}}{\theta_f} \right)^2 \sim L \sqrt{\frac{\omega}{\omega_c}}, \quad (2.18)$$

show that, for a given in-medium formation time τ_f , all the three time scales relevant for coherence depend solely upon the ratio $\theta_{q\bar{q}}/\theta_f$. Physically, this is a consequence of the fact that, at formation, the medium-induced gluon distribution (2.7) is characterized by the formation angle θ_f alone (for a given τ_f). Hence, when discussing interference effects, it is natural to distinguish between the values of $\theta_{q\bar{q}}$ which are larger than τ_f and those which are smaller. In addition, as we shall see, there is a change of regime when τ_{coh} becomes as large as the medium size L , which according to Eq. (2.17) happens when $\theta_{q\bar{q}} \simeq \theta_c$. We are thus led to consider the three following ranges for $\theta_{q\bar{q}}$:

1. **Relatively large dipole angles**, $\theta_f \lesssim \theta_{q\bar{q}} \lesssim \theta_s$. In this regime Eqs. (2.13), (2.15) and (2.16) imply the following hierarchy of scales

$$\tau_{int} \lesssim \tau_\lambda \lesssim \tau_{coh} \lesssim \tau_f \quad \text{when} \quad \theta_{q\bar{q}} \gtrsim \theta_f, \quad (2.19)$$

which shows that, for such large dipole angles, the condition (2.14) of quantum coherence is the most restrictive one. Accordingly, in this regime, the longitudinal phase-space for interferences is of order $\sim \tau_{int}\tau_f$ and thus is suppressed with respect to the corresponding phase-space $\sim \tau_f L$ for direct emissions by a factor

$$\mathcal{R} = \frac{\tau_{int}}{L} \sim \sqrt{\frac{\omega}{\omega_c}} \left(\frac{\theta_f}{\theta_{q\bar{q}}} \right)^2 \ll 1. \quad (2.20)$$

The range of values spanned by \mathcal{R} within this regime will be displayed in Eq. (5.17).

2. **Relatively small dipole angles** $\theta_c \ll \theta_{q\bar{q}} \ll \theta_f$. In this case, the strongest limitation on the phase-space for interference comes from the requirement of color coherence, as clear from the fact that the ordering of time scales is now reverted:

$$\tau_f \ll \tau_{coh} \ll \tau_\lambda \ll \tau_{int} \quad \text{when} \quad \theta_{q\bar{q}} \ll \theta_f. \quad (2.21)$$

So, the longitudinal phase-space for interference is now of order $\tau_{coh}\tau_f$. So long as $\theta_{q\bar{q}} \gg \theta_c$, this is still strongly suppressed as compared to the phase-space for direct emissions, as manifest from Eq. (2.17). Hence, in this regime too, the interference contribution to the spectrum is parametrically small (see also Eq. (5.18) for the corresponding range) :

$$\mathcal{R} = \frac{\tau_{coh}}{L} = \left(\frac{\theta_c}{\theta_{q\bar{q}}} \right)^{2/3} \ll 1. \quad (2.22)$$

Note that, in this case, the medium-induced radiation by the dipole (the incoherent sum of the two corresponding spectra by the quark and the antiquark) is distributed at large angles $\theta_q \simeq \theta_{\bar{q}} \gtrsim \theta_f \gg \theta_{q\bar{q}}$, that is, well outside the dipole cone. One may wonder why the total radiation in that case is not simply zero (as it would be for the large angle radiation by a color-singlet dipole in the vacuum). The reason is that, so long as $\theta_{q\bar{q}} \gg \theta_c$, a $q\bar{q}$ pair immersed in the medium is *not* a ‘color singlet’ anymore, except for a very brief period of time $\sim \tau_{coh}$.

3. **Very small dipoles angles** $\theta_{q\bar{q}} \lesssim \theta_c$. When the dipole angle is even smaller, $\theta_{q\bar{q}} \lesssim \theta_c$, the color coherence time τ_{coh} becomes as large as the medium size L , as clear from Eq. (2.17). In that case, the $q\bar{q}$ pair preserves its color and quantum coherence throughout the medium, so the interference effects are not suppressed anymore and they act towards reducing the medium-induced radiation by the dipole. For sufficiently small angles $\theta_{q\bar{q}} \ll \theta_c$, the color decoherence is parametrically small and the total (in-medium) radiation becomes negligible: the interference effects and the direct emissions nearly compensate each other³. This conclusion is in agreement⁴ with the results in [26], obtained by working to leading order in the ‘opacity expansion’ [13] — *i.e.* in the single scattering approximation — which is a legitimate approximation when $\theta_{q\bar{q}} \ll \theta_c$.

In summary, we have argued that for sufficiently large dipole angles $\theta_{q\bar{q}} \gg \theta_c$, the interference effects for the medium-induced radiation are negligible, so the total BDMPS-Z spectrum by the dipole is the incoherent sum of the respective spectra produced by the quark and the antiquark. For smaller angles $\theta_{q\bar{q}} \lesssim \theta_c$, the interference effects are not suppressed anymore and they eventually cancel the direct emissions when $\theta_{q\bar{q}} \ll \theta_c$. The transition between the two regimes, occurring at $\theta_{q\bar{q}} \simeq \theta_c$, could in principle be studied within the formalism that we shall develop later. However, such a study goes beyond the approximation schemes that we shall use throughout this paper and which are adapted to the most interesting regime at $\theta_{q\bar{q}} \gg \theta_c$.

Note that, although so far we have focused on gluons with relatively soft energies, $\omega \ll \omega_c$, our main conclusions remain valid when ω approaches the limiting value ω_c , as we now argue. When $\omega \sim \omega_c$, one has $\tau_f \sim L$ and $\theta_f \sim \theta_c$, so the intermediate regime of ‘relatively small dipole angles’ ceases to exist. Yet, Eq. (2.20) implies that, so long as $\theta_{q\bar{q}} \gg \theta_f(\omega_c) = \theta_c$, the interference effects are relatively small even for $\omega \sim \omega_c$. This is so because the time scale τ_{int} which limits quantum coherence is still much smaller than L in this regime.

We conclude our discussion by observing that the radiation of BDMPS-Z-like gluons is not the only medium induced radiation by the dipole. Indeed, in Ref [27], it has been shown that in the presence of a dense medium, leading to color decoherence over a distance of the order of the medium size L , the dipole produces additional soft gluon radiation, which is emitted outside of the medium and also outside the dipole cone ($\theta_q, \theta_{\bar{q}} > \theta_{q\bar{q}}$). As we shall further discuss in Sects. 3.2 and 6, this alternative mechanism operates only for relatively small dipole angles and the associated radiation is mostly collinear with the $q\bar{q}$ axis, in the sense that $\theta_q \sim \theta_{\bar{q}} \sim \theta_{q\bar{q}} \ll \theta_f$. Moreover, the associated gluon spectrum is simply the bremsstrahlung spectrum and hence it is independent of the medium size L . On the contrary, the medium-induced radiation that we consider is emitted at larger angles, within a range $\theta_f \lesssim \theta_q \lesssim \theta_s$, and it has a strength proportional to the medium length. Hence, these two mechanisms, which are simultaneously present in the medium, lead to gluon spectra with very small overlap.

3. General set-up and formalism

In this section, we shall more precisely describe our physical problem — a color dipole which radiates gluons while propagating through a QCD medium (say, a quark-gluon plasma) — and the formalism that we shall use in order to study the dipole interactions with the medium and its

³The net result should be of order $(\theta_{q\bar{q}}/\theta_c)^2$, as clear by inspection of Eq. (3.29) below.

⁴We would like to thank Carlos Salgado for useful discussions on this point.

Parameter	Definition	Parametric estimate	Physical meaning
τ_q	$\frac{2\omega}{k_\perp^2}$	$\tau_f \left(\frac{\theta_f}{\theta_q}\right)^2$	vacuum formation time
τ_f	$\sqrt{\frac{2\omega}{\hat{q}}}$	$\sqrt{\frac{\omega}{\omega_c}} L$	in-medium formation time
θ_f	$\left(\frac{2\hat{q}}{\omega^3}\right)^{1/4}$	$\theta_c \left(\frac{\omega_c}{\omega}\right)^{3/4}$	formation angle
θ_s	$\frac{\sqrt{\hat{q}L}}{\omega}$	$\theta_c \frac{\omega_c}{\omega}$	saturation angle
τ_{int}	$\frac{2}{\omega\theta_{q\bar{q}}^2}$	$\tau_f \left(\frac{\theta_f}{\theta_{q\bar{q}}}\right)^2$	interference time
τ_λ	$\frac{1}{\theta_{q\bar{q}}(\omega\hat{q})^{1/4}}$	$\tau_f \frac{\theta_f}{\theta_{q\bar{q}}}$	transverse resolution time
τ_{coh}	$\frac{2}{(\hat{q}\theta_{q\bar{q}}^2)^{1/3}}$	$\tau_f \left(\frac{\theta_f}{\theta_{q\bar{q}}}\right)^{2/3}$	color decoherence time

Table 1: Scales relevant for medium-induced gluon radiation. The dimensionless ratios are related to the BDMPS medium parameters $\omega_c = \hat{q}L^2/2$ and $\theta_c^2 = 1/\hat{q}L^3$

radiation. As noticed in the Introduction, a similar set-up has been also used in Refs. [26, 27]. But the focus there was on some special physical conditions, allowing for additional simplifications: the single scattering approximation (‘dilute medium’) in [26] and the restriction to out-of-medium emissions (‘soft and collinear gluons’) in [27]. Here, we shall keep our discussion as general as possible, in such a way to encompass the physics of medium-induced gluon radiation in the multiple soft scattering regime. In the process, we shall also make contact with the results in Ref. [27] and thus clarify the precise kinematical region for their applicability.

3.1 The amplitude for gluon emission

The in-medium dipole dynamics will be treated in the semi-classical approximation, that is, by solving classical equations of motion in which the dipole enters as a classical source of color charge. The medium rescattering will be resummed to all orders via a background field method. The effects of this rescattering on the quark and the antiquark legs of the dipole will be treated in the eikonal approximation. The corresponding effects on the emitted gluon will be treated exactly (within the semi-classical approximation), by using an appropriate background field propagator. The background field is assumed to be random, with a Gaussian distribution, and the average over its fluctuations will be performed using techniques borrowed from the color glass condensate [31]. The underlying assumptions are that the two quarks are very energetic, with momenta much larger than any momentum which can be transferred by the medium, whereas the emitted gluon carries (transverse) momenta comparable to those of the medium. Under these assumptions, our calculations are correct to lowest order in the color charge of the dipole but to all orders in the medium effects. This formalism has been used in Ref. [32] to study the radiation by a single quark and shown to encompass the essential BDMPS-Z physics.

The *color dipole* is truly a pair of classical, massless, particles with opposite color charges (so that the pair is a color singlet) which is produced at time $t_0 = 0$ by some hard process occurring

inside the medium. After being produced, the two particles separate from each other at constant velocities, $\mathbf{u} = \mathbf{p}_q/E_q$ for the quark (q) and $\bar{\mathbf{u}} = \mathbf{p}_{\bar{q}}/E_{\bar{q}}$ for the antiquark (\bar{q}), which make a relative angle $\theta_{q\bar{q}} : \mathbf{u} \cdot \bar{\mathbf{u}} = \cos \theta_{q\bar{q}}$. Here \mathbf{p}_q and $E_q = |\mathbf{p}_q|$ represent the 3-momentum and the energy of the quark (and similarly for the antiquark), assumed to be much larger than any other momentum scale in the problem. The only way that the medium can act on such an energetic particle is by inducing a *color precession* (see below). We choose the longitudinal axis (x^3) as the direction of motion of the center-of-mass of the $q\bar{q}$ pair. In the medium rest frame, the dipole has a relatively large longitudinal boost $\gamma \gg 1$ and hence a relatively small opening angle $\theta_{q\bar{q}} \sim 1/\gamma$. This angle will be nevertheless assumed to be significantly larger than the critical angle for medium-induced radiation $\theta_c \sim 1/(Q_s L)$, which is very small ($\theta_c \ll 1$) as explained in the previous section. The dipole propagates through the medium along a longitudinal distance L before escaping into the vacuum.

The *QCD medium* is described as a random color background field \mathcal{A}_a^μ with a Gaussian distribution. As well known e.g. from the experience with the color glass condensate [31], this description becomes simpler by working in a Lorentz frame in which the medium is strongly boosted (an ‘infinite momentum frame’). For the problem at hand, it is convenient to choose the ‘dipole frame’ in which the COM of the $q\bar{q}$ pair is nearly at rest, meaning that the plasma is boosted (essentially, by the dipole γ factor introduced above) in the negative x^3 direction. In this new frame and in light-cone (LC) gauge $A_a^+ = 0$, the background field has only one non-trivial component, $\mathcal{A}_a^\mu = \delta^{\mu-} \mathcal{A}_a^-$, which is moreover independent of the LC ‘time’ x^- , by Lorentz time dilation. We have introduced here the LC components of the 4-vector \mathcal{A}_a^μ , defined in the standard way; e.g. $x^\mu = (x^+, x^-, \mathbf{x}_\perp)$, with

$$x^+ = \frac{1}{\sqrt{2}}(x^0 + x^3), \quad x^- = \frac{1}{\sqrt{2}}(x^0 - x^3), \quad \mathbf{x}_\perp = (x^1, x^2). \quad (3.1)$$

In the dipole frame, both the dipole angle $\theta_{q\bar{q}}$ and the characteristic medium angle θ_c are enhanced by a factor γ (so, in particular, $\theta_{q\bar{q}} \sim \mathcal{O}(1)$), but the inequality $\theta_{q\bar{q}} \gg \theta_c$ remains of course true. In view of that, and in order to avoid a proliferation of symbols, we shall use the same notations for quantities in the plasma rest frame and in the dipole frame — the difference should be clear from the context. Moreover, we shall often use the small-angle version of a parametric estimate (e.g., $\tau_q \simeq 2/\omega\theta_q^2$) even when working in the boosted frame, where the angles are not necessarily small; what we truly mean by such a writing, is an estimate which becomes true after boosting back to the plasma rest frame.

Another advantage of using the dipole frame refers to the correlations between the charged constituents of the medium (say, quark and gluon quasiparticles in the case of a weakly-coupled QGP): the longitudinal (x^+) range of the correlations, which was $1/\mu_D$ in the original frame, is now Lorentz-contracted to $1/(\gamma\mu_D)$. When probing this distribution over relatively large longitudinal separations $\Delta x^+ \gg 1/(\gamma\mu_D)$, one can describe the medium constituents as independent color charges with a current density $J_{\text{med}}^{\mu,a}(x) = \delta^{\mu-} \rho^a(x^+, \mathbf{x}_\perp)$ and a local 2-point correlation

$$\langle \rho^a(x^+, \mathbf{x}_\perp) \rho^b(y^+, \mathbf{y}_\perp) \rangle = \delta^{ab} \delta(x^+ - y^+) \delta^{(2)}(\mathbf{x}_\perp - \mathbf{y}_\perp) n_0, \quad (3.2)$$

where n_0 is the average color charge squared per unit volume, assumed to be homogeneous. (For a longitudinally expanding medium, this would be a function of x^+ .) If the medium is a QGP,

then $n_0 \propto \gamma T \mu_D^2$ in the dipole frame. Such a color charge distribution gives rise to the following distribution for the background field \mathcal{A}_a^- :

$$\langle \mathcal{A}_a^-(x^+, \mathbf{q}_\perp) \mathcal{A}_b^-(y^+, \mathbf{k}_\perp) \rangle = \delta_{ab} \delta(x^+ - y^+) (2\pi)^2 \delta^{(2)}(\mathbf{q}_\perp - \mathbf{k}_\perp) \frac{n_0}{(q_\perp^2 + \mu_D^2)^2}. \quad (3.3)$$

Note that the Debye screening has been heuristically implemented as a ‘gluon mass’ μ_D , although the actual mechanisms at work are generally more complicated.

The *gluon radiation* by the dipole will be described in the classical approximation, as the additional color field (on top of the background field) generated by the $q\bar{q}$ pair. The classical approximation is correct when the gluon is soft relative to its sources, meaning that $\omega = |\mathbf{k}| \ll E_q, E_{\bar{q}}$. The color field a_a^μ describing the radiation is a small perturbation of the background field and will be obtained by solving the linearized version of the Yang–Mills equation for the total field $A^\mu = \delta^{\mu-} \mathcal{A}^- + a^\mu$ (color indices will be often kept implicit in what follows)

$$D_\nu F^{\nu\mu} = \delta^{\mu-} \rho + J_{\text{dip}}^\mu. \quad (3.4)$$

The dipole color current $J_{\text{dip}}^\mu = J_q^\mu + J_{\bar{q}}^\mu$ involves contributions from the quark and the antiquark and also depends upon the background field, because it obeys a covariant conservation law: $\mathcal{D}_\mu J_{\text{dip}}^\mu = 0$, where $\mathcal{D}^\mu = \partial^\mu + \delta^{\mu-} ig \mathcal{A}^-$.

In the vacuum ($\mathcal{A}^- = 0$), the color current associated with a pair of classical particles with constant velocities can be written as $j_{\text{dip}}^\mu = j_q^\mu + j_{\bar{q}}^\mu$, with

$$\begin{aligned} j_{q,a}^\mu(x) &= g u^\mu \theta(x^+) \delta(x^- - u^- x^+) \delta^{(2)}(\mathbf{x}_\perp - \mathbf{u}_\perp x^+) \mathcal{C}_a, \\ j_{\bar{q},a}^\mu(x) &= -g \bar{u}^\mu \theta(x^+) \delta(x^- - \bar{u}^- x^+) \delta^{(2)}(\mathbf{x}_\perp - \bar{\mathbf{u}}_\perp x^+) \mathcal{C}_a. \end{aligned} \quad (3.5)$$

We have used here LC notations, with $u^\mu \equiv p_q^\mu/p_q^+ = (1, u^-, \mathbf{u}_\perp)$ and $\bar{u}^\mu \equiv p_{\bar{q}}^\mu/p_{\bar{q}}^+ = (1, \bar{u}^-, \bar{\mathbf{u}}_\perp)$. Note that for the right–moving dipole, x^+ plays the role of ‘time’ while x^- is the ‘longitudinal coordinate’. The ‘color charges’ \mathcal{C}_a are the components of a color vector in the adjoint representation describing the orientation of the quark current in the internal $\text{SU}(N_c)$ space; for the antiquark, $\bar{\mathcal{C}}_a = -\mathcal{C}_a$. The current is conserved, $\partial_\mu j_{\text{dip}}^\mu = 0$, since $\partial_\mu j_{q,a}^\mu = g \mathcal{C}_a \delta^{(4)}(x) = -\partial_\mu j_{\bar{q},a}^\mu$.

In the eikonal approximation, the effect of the medium on the dipole consists merely in color rotations, separately for the quark and the antiquark:

$$J_{q,a}^\mu(x) = \mathcal{U}_q^{ab}(x^+, 0) j_{q,a}^\mu(x), \quad J_{\bar{q},a}^\mu(x) = \mathcal{U}_{\bar{q}}^{ab}(x^+, 0) j_{\bar{q},a}^\mu(x). \quad (3.6)$$

$\mathcal{U}_q(x^+, 0)$ is a Wilson line in the adjoint representation, which is the special case of

$$\mathcal{U}(x^+, y^+; [\mathbf{r}_\perp]) = \text{P exp} \left\{ -ig \int_{y^+}^{x^+} dz^+ \mathcal{A}^-(z^+, \mathbf{r}_\perp(z^+)) \right\} \quad (3.7)$$

for $y^+ = 0$ and the transverse path $\mathbf{r}_\perp(z^+) = \mathbf{u}_\perp z^+$ (the quark trajectory in the transverse plane). In Eq. (3.7), $\mathcal{A}^- = \mathcal{A}_a^- T^a$ is a color matrix in the adjoint representation and the symbol P denotes time–ordering in z^+ . Using $(\partial/\partial x^+) \mathcal{U}_q^{ab} = -ig \mathcal{A}_{ac}^-(x) \mathcal{U}_q^{cb}$, it is easy to check that $\mathcal{D}_\mu J_{q,a}^\mu = g \mathcal{C}_a \delta^{(4)}(x) = -\mathcal{D}_\mu J_{\bar{q},a}^\mu$, so the dipole current is *covariantly* conserved, as it should. Note that, although the wavefunction of a physical quark is known to transform according to the *fundamental* representation of the color group, the corresponding color current (3.6) involves a

Wilson line in the *adjoint* representation, since this current is a vector in the color space $SU(N_c)$. The only trace of the underlying fundamental representation lies in the normalization of the color vector \mathcal{C}_a , namely $\mathcal{C}_a \mathcal{C}_a = C_F = (N_c^2 - 1)/2N_c$.

In the LC gauge $A^+ = 0$, only the transverse components a^i (with $i = 1, 2$) of the radiated field contribute to the matrix element for gluon emission (see below). The corresponding, linearized, equation of motion is readily obtained from Eq. (3.4) and reads

$$(2\partial^+ \mathcal{D}^- - \nabla_\perp^2) a^i = J_{\text{dip}}^i - \frac{\partial^i}{\partial^+} J_{\text{dip}}^+. \quad (3.8)$$

This equation can be formally solved in terms of the background field Klein–Gordon propagator, *i.e.* the Green’s function for the differential operator in the left hand side. The corresponding solution is well known in the literature (see e.g. [32]) and will be succinctly described here. Given that the background field is independent of x^- , it is convenient to first perform a Fourier transform to the k^+ representation. Then the solution to Eq. (3.8) can be written as

$$a_a^i(x^+, \mathbf{x}_\perp; k^+) = \frac{i}{2k^+} \int dy^+ d\mathbf{y}_\perp \mathcal{G}_{ab}(x^+, \mathbf{x}_\perp; y^+, \mathbf{y}_\perp; k^+) \mathcal{J}_b^i(y^+, \mathbf{y}_\perp; k^+), \quad (3.9)$$

where \mathcal{J}^i refers to the total current in the r.h.s. of Eq. (3.8) and the Green’s function \mathcal{G} obeys

$$\left(i\mathcal{D}^- + \frac{\nabla_\perp^2}{2k^+} \right) \mathcal{G}(x^+, \mathbf{x}_\perp; y^+, \mathbf{y}_\perp; k^+) = i\delta(x^+ - y^+) \delta^{(2)}(\mathbf{x}_\perp - \mathbf{y}_\perp). \quad (3.10)$$

\mathcal{G} is formally the same as the $D = 2+1$ Schrödinger evolution operator for a quantum–mechanical particle with mass k^+ and time x^+ propagating in a time–dependent potential $g\mathcal{A}^-$. As well known, this propagator admits the following representation as a path integral:

$$\mathcal{G}(x^+, \mathbf{x}_\perp; y^+, \mathbf{y}_\perp; k^+) = \int [D\mathbf{r}_\perp(z^+)] \exp \left\{ i \frac{k^+}{2} \int_{y^+}^{x^+} dz^+ \dot{\mathbf{r}}_\perp^2(z^+) \right\} \mathcal{U}(x^+, y^+; [\mathbf{r}_\perp]), \quad (3.11)$$

with the paths $\mathbf{r}_\perp(z^+)$ obeying the boundary conditions $\mathbf{r}_\perp(y^+) = \mathbf{y}_\perp$ and $\mathbf{r}_\perp(x^+) = \mathbf{x}_\perp$. The corresponding vacuum propagator ($\mathcal{A}^- = 0$) will be also needed :

$$\mathcal{G}_0(x^+, \mathbf{x}_\perp; y^+, \mathbf{y}_\perp; k^+) = \Theta(x^+ - y^+) \frac{k^+}{2\pi i(x^+ - y^+)} \exp \left\{ i \frac{k^+ (\mathbf{x}_\perp - \mathbf{y}_\perp)^2}{2(x^+ - y^+)} \right\}. \quad (3.12)$$

Note that Eq. (3.11) goes beyond the eikonal approximation in the sense that the gluon trajectory is not *a priori* imposed (as we did for the quark and the antiquark), but rather is determined by the gluon interactions with the background field.

Given the solution a^i , the gluon emission amplitude is obtained as (for an on–shell gluon with 4–momentum k^μ , color a , and polarization λ)

$$\mathcal{M}_\lambda^a(k^+, \mathbf{k}_\perp) = - \lim_{k^2 \rightarrow 0} k^2 a_\mu^a(k) \epsilon_\lambda^\mu(k), \quad \epsilon_\lambda^\mu(k^+, \mathbf{k}_\perp) = \left(0, \frac{\boldsymbol{\epsilon}_\perp \cdot \mathbf{k}_\perp}{k^+}, \boldsymbol{\epsilon}_\perp \right). \quad (3.13)$$

In the LC gauge $a^+ = 0$, this involves only the transverse components a^i , as anticipated. Using Eq. (3.9) for $x^+ \rightarrow \infty$ together with the following composition law (valid for $x^+ > z^+ > y^+$)

$$\mathcal{G}(x^+, \mathbf{x}_\perp; y^+, \mathbf{y}_\perp; k^+) = \int d\mathbf{z}_\perp \mathcal{G}(x^+, \mathbf{x}_\perp; z^+, \mathbf{z}_\perp; k^+) \mathcal{G}(z^+, \mathbf{z}_\perp; y^+, \mathbf{y}_\perp; k^+), \quad (3.14)$$

applied to $z^+ = L^+ \equiv \sqrt{2}L$ (notice that for $x^+ > L^+$, one has $\mathcal{A}^- = 0$ and then $\mathcal{G} = \mathcal{G}_0$), one obtains the amplitude as a sum of two pieces,

$$\mathcal{M}_a^i(k^+, \mathbf{k}_\perp) \equiv - \lim_{k^2 \rightarrow 0} k^2 a_a^i(k) = \mathcal{M}_a^{i,\text{in}} + \mathcal{M}_a^{i,\text{out}}, \quad (3.15)$$

describing emissions inside the medium ($0 < x^+ < L^+$) and outside the medium ($x^+ > L^+$), respectively. Each of these pieces is a sum of quark and antiquark contributions and below we only show the respective quark contributions. The ‘out’ piece is the simplest:

$$\begin{aligned} \mathcal{M}_{a,q}^{i,\text{out}}(k^+, \mathbf{k}_\perp) &= \int d^4x e^{ik \cdot x} \Theta(x^+ - L^+) \mathcal{J}_{a,q}^i(x) \\ &= g(u^i - v^i) \mathcal{U}_q^{ab}(L^+, 0) \mathcal{C}_b \int_{L^+}^{\infty} dx^+ e^{i(k \cdot u)x^+} \end{aligned} \quad (3.16)$$

where $k^- = \mathbf{k}_\perp^2/2k^+$, $\mathcal{J}_q^i = J_q^i - (\partial^i/\partial^+)J_q^+$, and in the second line we have used the δ -functions in Eq. (3.5) to perform the integrations over x^- and \mathbf{x}_\perp and denoted $v^\mu \equiv k^\mu/k^+ = (1, v^-, \mathbf{v}_\perp)$. The ‘in’ piece of the quark–emission amplitude reads

$$\begin{aligned} \mathcal{M}_{a,q}^{i,\text{in}}(k^+, \mathbf{k}_\perp) &= g \int_0^{L^+} dx^+ e^{ik^-L^+ + i(k^+u^-)x^+} \int d\mathbf{z}_\perp e^{-i\mathbf{k}_\perp \cdot \mathbf{z}_\perp} \\ &\quad (u^i + i\partial_x^i/k^+) \mathcal{G}_{ab}(L^+, \mathbf{z}_\perp; x^+, \mathbf{x}_\perp; k^+) \Big|_{\mathbf{x}_\perp = \mathbf{u}_\perp x^+} \mathcal{U}_q^{bc}(x^+, 0) \mathcal{C}_c. \end{aligned} \quad (3.17)$$

The corresponding formulæ for the antiquark are obtained by replacing $u^\mu \rightarrow \bar{u}^\mu$ and $\mathcal{C}_a \rightarrow -\mathcal{C}_a$.

Given the amplitude, the emission probability \mathcal{P} and the gluon spectrum are obtained by taking the modulus squared and then summing over colors and polarizations:

$$\omega \frac{dN}{d^3\mathbf{k}} = \frac{1}{16\pi^3} \mathcal{P}(\mathbf{k}), \quad \mathcal{P}(\mathbf{k}) \equiv \sum_{a,i} \langle |\mathcal{M}_a^i|^2 \rangle, \quad (3.18)$$

where we have written the gluon momentum in normal coordinates as $k^\mu = (\omega, \mathbf{k})$ with $\omega = |\mathbf{k}|$ and performed the polarization sum by using $\sum_\lambda \epsilon_\lambda^i(k) \epsilon_\lambda^{j*}(k) = \delta^{ij}$. The brackets in Eq. (3.18) refer to the medium average according to Eq. (3.3).

The amplitude \mathcal{M}_a^i is truly a sum of four terms: (q, in) , (q, out) , (\bar{q}, in) , and (\bar{q}, out) . Hence the emission probability in Eq. (3.18) involves 16 terms: 8 of them describe direct emissions by either the quark or the antiquark, and 8 represent $q\bar{q}$ interference terms. Each of these types of contributions — direct or interference — involves three types of pieces: (in, in), (in, out), or (out, out). For the (in, in) contributions, the gluon is emitted inside the medium in both the direct amplitude and the complex conjugate one⁵; denoting the respective emission times as x^+ and y^+ , we have $0 < x^+, y^+ < L^+$. For the (in, out) terms, one has $0 < x^+ < L^+$ and $y^+ > L^+$, or vice-versa. Finally, for the (out, out) pieces, both x^+ and y^+ are larger than L^+ .

We anticipate that, for the problem of medium–induced gluon radiation, the (in, in) contributions will be the most important ones, both for direct emissions and for the interference terms. Here, however, we shall start by computing the respective (out, out) pieces, with the purpose of illustrating the medium averaging and the phenomenon of color decoherence in the simplest possible setting. This will also allow us to make contact with the results in Ref. [27].

⁵It would be perhaps more appropriate to say that the gluon is *emitted* in the direct amplitude and *reabsorbed* in the complex conjugate amplitude. For brevity, we shall refer to all such processes as ‘emissions’.

3.2 The ‘out–out’ terms as a warm up

Consider first the direct gluon emission, say from the quark. Eq. (3.16) implies

$$\begin{aligned} \mathcal{P}_q^{(\text{out})}(\mathbf{k}) &= g^2(\mathbf{u}_\perp - \mathbf{v}_\perp)^2 \langle \mathcal{U}_q^{ab}(L^+, 0) \mathcal{C}_b \mathcal{C}_d \mathcal{U}_q^{\dagger ad}(L^+, 0) \rangle \int_{L^+}^\infty dx^+ \int_{L^+}^\infty dy^+ e^{i(k \cdot u)(x^+ - y^+)} \\ &= g^2 C_F \frac{(\mathbf{u}_\perp - \mathbf{v}_\perp)^2}{(k \cdot u)^2} = \frac{2g^2 C_F}{(k^+)^2} \frac{1}{v \cdot u}, \end{aligned} \quad (3.19)$$

where the second line follows after using $\mathcal{C}_b \mathcal{C}_d = \delta_{bd} C_F / (N_c^2 - 1)$ — the condition that prior to the emission the $q\bar{q}$ pair be in a color singlet state. We have also used (recall that e.g. $v^\mu = (1, v^-, \mathbf{v}_\perp)$ with $v^2 = 0$ and hence $2v^- = \mathbf{v}_\perp^2$)

$$(\mathbf{u}_\perp - \mathbf{v}_\perp)^2 = \mathbf{u}_\perp^2 + \mathbf{v}_\perp^2 - 2\mathbf{u}_\perp \cdot \mathbf{v}_\perp = 2(u^- + v^- - \mathbf{u}_\perp \cdot \mathbf{v}_\perp) = 2v \cdot u. \quad (3.20)$$

An expression similar to Eq. (3.21) but with $v \cdot u \rightarrow v \cdot \bar{u}$ holds for the direct emission by the antiquark. Note that there is no medium dependence in the final result for $\mathcal{P}_q^{(\text{out})}$ because (1) the quark Wilson lines in the direct and the complex conjugate amplitude have compensated each other, and (2) there was a similar cancelation of the L -dependent phases $e^{\pm i(k \cdot u)L^+}$ generated by the lower limit L^+ of the time integrations. Accordingly, Eq. (3.21) is formally identical to the corresponding probability in the vacuum, $\mathcal{P}_q^{(\text{vac})}$. For later use, it is convenient to rewrite this vacuum probability as

$$\mathcal{P}_q^{(\text{vac})}(\mathbf{k}) = 2g^2 C_F (\mathbf{u}_\perp - \mathbf{v}_\perp)^2 \tau_q^2, \quad (3.21)$$

where we have recognized the formation time (for an emission by the quark) $\tau_q = 1/[\sqrt{2}(k \cdot u)]$. Indeed, in a frame where the quark propagates along the longitudinal axis ($\mathbf{u}_\perp = 0$), one has $k \cdot u = k^- = k_\perp^2 / 2k^+$, which is the inverse formation time adapted to the LC time variable x^+ . More generally, in the actual frame where the quark has a transverse velocity \mathbf{u}_\perp , we can write

$$k \cdot u = \frac{\omega E_q}{p_q^+} (1 - \cos \theta_q) \simeq \frac{\omega \theta_q^2}{2\sqrt{2}} \implies \tau_q = \frac{1}{\sqrt{2}(k \cdot u)} \simeq \frac{2}{\omega \theta_q^2}, \quad (3.22)$$

where one recognizes the expression (2.1) for the formation time at small angles. In writing Eq. (3.22) we performed approximations valid when all the angles in the problem (the dipole angle and the gluon emission angles) are small; then $p_q^+ \simeq \sqrt{2}E_q$ etc. In what follows we shall systematically perform such approximations which are strictly valid in the plasma rest frame.

As explained in Sect. 2, throughout this paper we are mostly interested in emissions at relatively large angles, for which the formation times are small: $\tau_q \ll L^+$. On the other hand, the (out, out) piece (3.19) of the emission probability is controlled, by construction, by emission times x^+ and y^+ within the range $L^+ \leq x^+, y^+ \lesssim L^+ + \tau_q$, which are much larger than τ_q . It would be very unnatural that gluons be emitted (in the vacuum) at times much larger than their formation times. But as a matter of facts, when $\tau_q \ll L^+$ there is no *physical* out–of–medium emission; in that case, Eq. (3.19) represents merely a piece of the total result which cancels against other pieces. More precisely, the boundary terms generated by emission times within an interval $\Delta x^+ \simeq \tau_q$ around the medium boundary at L^+ cancel among the (in, in), (in, out), and (out, out) contributions, separately for the direct emissions and for the interference terms.

The net result is that all the *vacuum-like* emissions at large angles are emitted at early times $x^+, y^+ \lesssim \tau_q \ll L^+$, as expected on physical grounds.

The above argument also explains why the (out, out) pieces play no physical role for the situation of interest in this paper, which is characterized by small formation times: $\tau_q, \tau_{\bar{q}} \ll L$. On the other hand, these pieces become important for the relatively soft and collinear emissions which have large formation times $\tau_q, \tau_{\bar{q}} \gtrsim L$. This is the situation considered in Ref. [27]. To make contact with the results in that paper, we shall now consider the (out, out) contribution to the interference term. From Eq. (3.16), this is obtained as

$$\mathcal{I}^{(\text{out})}(\mathbf{k}) = -\frac{2g^2 C_F}{(k^+)^2} \frac{(u^i - v^i)(\bar{u}^i - v^i)}{(v \cdot u)(v \cdot \bar{u})} \cos[L^+ k \cdot (u - \bar{u})] S_{q\bar{q}}(L^+, 0), \quad (3.23)$$

where the quark and the antiquark Wilson lines combined in the following 2–point function

$$S_{q\bar{q}}(L^+, 0) = \frac{1}{N_c^2 - 1} \langle \text{Tr} \mathcal{U}_q(L^+, 0) \mathcal{U}_{\bar{q}}^\dagger(L^+, 0) \rangle, \quad (3.24)$$

which describes the residual color coherence between the two fermions after having crossed the medium — that is, the probability for the $q\bar{q}$ pair to remain in a color singlet state. $S_{q\bar{q}}$ is formally the same as the scattering S –matrix for a dipole made with a pair of colored particles in the adjoint representation that we shall succinctly refer to as the ‘ $q\bar{q}$ dipole’. For a background field with a Gaussian distribution, cf. Eq. (3.3), the expectation value in Eq. (3.24) is easily computed as (see e.g. [31])

$$S_{\text{dip}}(x^+, y^+; [\mathbf{r}_\perp]) = \exp \left\{ -g^2 N_c \int_{y^+}^{x^+} dz^+ n_0(z^+) \int \frac{d^2 \mathbf{q}_\perp}{(2\pi)^2} \frac{1 - e^{i\mathbf{q}_\perp \cdot \mathbf{r}_\perp(z^+)}}{(\mathbf{q}_\perp^2 + \mu_D^2)^2} \right\}, \quad (3.25)$$

where for later convenience we have kept generic endpoints in time, y^+ and x^+ , and a generic ‘trajectory’ $\mathbf{r}_\perp(z^+)$ for the dipole transverse size in the interval $y^+ < z^+ < x^+$. For the cases of interest in this work, the dipole size is always much smaller than the medium screening length, $r \equiv |\mathbf{r}_\perp| \ll \mu_D^{-1}$. Then the integral over \mathbf{q}_\perp in Eq. (3.25) is controlled by transverse momenta within the range $\mu_D < q_\perp < 1/r$ and to leading logarithmic accuracy it can be estimated by expanding $e^{i\mathbf{q}_\perp \cdot \mathbf{r}_\perp}$ to second order. This yields

$$S_{\text{dip}}(x^+, y^+; [\mathbf{r}_\perp]) \simeq \exp \left\{ -\frac{\alpha_s N_c}{4} \int_{y^+}^{x^+} dz^+ n_0(z^+) r^2(z^+) \ln \frac{1}{r^2(z^+) \mu_D^2} \right\}, \quad (3.26)$$

where the logarithm $\rho \equiv \ln(1/r^2 \mu_D^2)$ is assumed to be relatively large, $\rho \gg 1$. A more compact version of Eq. (3.26) can be obtained by assuming $n_0(z^+) = n_0$ to be constant and neglecting the variation of the logarithm within the interval of integration; then,

$$S_{\text{dip}}(x^+, y^+; [\mathbf{r}_\perp]) \simeq \exp \left\{ -\frac{1}{4} \hat{q} \rho \int_{y^+}^{x^+} dz^+ r^2(z^+) \right\}, \quad (3.27)$$

where (the saturation scale Q_s is introduced for later reference)

$$\hat{q} \equiv \alpha_s N_c n_0 \sim \alpha_s N_c \mu_D^2 T, \quad Q_s^2 \equiv \hat{q} L^+, \quad (3.28)$$

and it is understood that the logarithm ρ in Eq. (3.27) is evaluated with the maximal dipole size r_{\max} within the interval $y^+ < z^+ < x^+$. (Eqs. (3.28) and (2.3) are consistent with each other since $\ell \sim 1/(\alpha_s N_c T)$ for a weakly-coupled QGP.)

When applying these formulæ to the $q\bar{q}$ dipole in Eq. (3.24), one has $\mathbf{r}_\perp(z^+) = (\mathbf{u}_\perp - \bar{\mathbf{u}}_\perp)z^+$ with $0 < z^+ < L^+$ and therefore

$$S_{q\bar{q}}(L^+, 0) \simeq \exp\left\{-\frac{1}{12}\hat{q}\rho(\mathbf{u}_\perp - \bar{\mathbf{u}}_\perp)^2(L^+)^3\right\} \simeq \exp\left\{-\frac{1}{24}(Q_s\theta_{q\bar{q}}L^+)^2\rho\right\}, \quad (3.29)$$

where in writing the second estimate we have used a small-angle approximation which holds, strictly speaking, in the plasma rest frame (the product $\theta_{q\bar{q}}L^+$ is boost invariant):

$$(\mathbf{u}_\perp - \bar{\mathbf{u}}_\perp)^2 = 2\mathbf{u} \cdot \bar{\mathbf{u}} = 2\frac{p_q \cdot p_{\bar{q}}}{p_q^+ p_{\bar{q}}^+} = 2\frac{E_q E_{\bar{q}}}{p_q^+ p_{\bar{q}}^+} (1 - \cos\theta_{q\bar{q}}) \simeq \frac{\theta_{q\bar{q}}^2}{2}. \quad (3.30)$$

At this point one should recall that we consider a relatively large dipole angle, $\theta_{q\bar{q}} \gg \theta_c$ or $Q_s\theta_{q\bar{q}}L^+ \gg 1$. The exponent in Eq. (3.29) is therefore large, which implies that $S_{q\bar{q}} \ll 1$. We see that the (out, out) contribution to interference is washed out by the medium, due to the color decoherence suffered by the $q\bar{q}$ pair after passing through the medium: since they move along different directions, the quark and the antiquark undergo different color precessions, so after leaving the medium, they do not form a color singlet anymore. Since the interference term vanishes, it follows that *in the regime where the (out, out) piece yields a physical contribution*, the total dipole radiation is the incoherent sum of two vacuum-like contributions (cf. Eq. (3.19)), by the quark and the antiquark. This is the main conclusion in Ref. [27] and admits interesting consequences: it implies that, in the presence of the medium, there should be an enhancement in the radiation at large angles, outside the dipole cone: $\theta_q, \theta_{\bar{q}} > \theta_{q\bar{q}}$.

To fully appreciate the impact of this conclusion, it is important to specify the kinematical region where it applies. From the previous arguments, it is clear that this relies on two main assumptions: (i) relatively large formation times⁶ $\tau_q, \tau_{\bar{q}} \gtrsim L$, and (ii) a sufficiently large dipole angle $\theta_{q\bar{q}} \gg \theta_c$. As we shall now argue, these conditions are satisfied for sufficiently soft gluons and for relatively small, but not too small, emission ($\theta_q, \theta_{\bar{q}}$) and dipole ($\theta_{q\bar{q}}$) angles. The precise conditions read

$$\omega \ll \omega_c \quad \text{and} \quad \theta_c \ll \theta_q, \theta_{\bar{q}}, \theta_{q\bar{q}} \lesssim \theta_c \left(\frac{\omega_c}{\omega}\right)^{1/2}. \quad (3.31)$$

The upper limit on ω comes up by combining the two conditions above and focusing on emission angles which are commensurable with the dipole angle: $\theta_q \sim \theta_{\bar{q}} \sim \theta_{q\bar{q}}$ (this is the regime where the conclusion in Ref. [27] have non-trivial consequences). Then, one can write

$$\tau_q \simeq \frac{2}{\omega\theta_q^2} \gtrsim L \quad \implies \quad \omega \lesssim \frac{2}{L\theta_{q\bar{q}}^2} \ll \frac{2}{L\theta_c^2} = \omega_c, \quad (3.32)$$

where we have used $\theta_q \sim \theta_{q\bar{q}} \gg \theta_c$ and $\theta_c^2 = 2/(\omega_c L)$, cf. Eq. (2.5). Then the upper limit on the values of the angles follows by rewriting the condition $\tau_q \gtrsim L$ in the form

$$\theta_q \lesssim \sqrt{\frac{2}{\omega L}} = \theta_c \sqrt{\frac{\omega_c}{\omega}}. \quad (3.33)$$

⁶Formally, this condition is necessary to avoid the rapid oscillations of the cosine factor in Eq. (3.23), whose argument is the same as $L^+k \cdot (u - \bar{u}) = L/\tau_q - L/\tau_{\bar{q}}$. Less formally, the regime of large formation times $\gtrsim L$ is the only one where the (out, out) piece of the spectrum is physically irrelevant, as already explained.

It should be also clear from the above that for a very small dipole angle $\theta_{q\bar{q}} \lesssim \theta_c$, the medium effects become irrelevant (since the $q\bar{q}$ pair preserves its color coherence throughout the medium), so the soft emissions with $\tau_q \gtrsim L$ proceed exactly as in the vacuum — in particular, the dipole antenna shows the characteristic angular ordering.

Note that the region (3.31) has some overlap with the ‘small-angle regime’ for medium-induced gluon radiation as defined in Sect. 2.2 — that is, the regime characterized by $\theta_c \ll \theta_{q\bar{q}} \ll \theta_f$. There is, however, an important difference: the respective range in Sect. 2.2 refers to the *dipole* angle $\theta_{q\bar{q}}$ alone; while this angle can be as small as θ_c , the actual *emission* angles for the BDMPS-Z gluons are much larger: $\theta_q, \theta_{\bar{q}} \gtrsim \theta_f \gg \theta_c$. On the other hand, the upper limit in Eq. (3.31) is much smaller than θ_f , as it can be easily checked using Eq. (2.9). So, even for dipole angles $\theta_{q\bar{q}}$ as small as shown in Eq. (3.31), the out-of-medium emissions discussed in Ref. [27] and the BDMPS-Z-like emissions that we presently focus on are geometrically separated, with the latter being distributed at significantly larger angles than the former.

4. Medium-induced gluon radiation: direct emission

Starting with this section, we shall concentrate on the in-medium, or (in, in), pieces, which are the dominant contributions to medium-induced gluon radiation in the kinematical range of interest (relatively small frequencies, $\omega \ll \omega_c$, or large emission angles $\theta_q \gtrsim \theta_f(\omega) \gg \theta_c$, cf. Eq. (2.9)). Although we are ultimately interested in the quark-antiquark interference terms, for which we shall present original results in the next section, here we shall start our analysis with the direct emission terms, from which we shall extract the BDMPS-Z spectrum. This will give us the opportunity to develop a series of approximations that we shall test on the case of direct emissions and then apply to the interference terms. These approximations, which are correct to parametric accuracy, have the virtue to render the physical interpretation transparent and thus allow us to pinpoint the subtle mechanisms at work in the interference effects. More precise calculations will be presented in Appendix A and they will confirm the results in this and the next coming section to the accuracy of interest.

The probability for in-medium gluon radiation by the quark is obtained by taking the modulus squared of the amplitude (3.17), summing over the final color indices, averaging over the initial ones, and performing the medium average over the background field. This yields

$$\begin{aligned} \mathcal{P}_q^{(\text{in})}(\mathbf{k}) &= 2g^2 C_F \text{Re} \int_0^{L^+} dx^+ \int_0^{x^+} dy^+ e^{ik^+u^-(x^+-y^+)} \\ &\quad \times \int d\mathbf{z}_{1\perp} \int d\mathbf{z}_{2\perp} e^{-i\mathbf{k}_\perp \cdot (\mathbf{z}_{1\perp} - \mathbf{z}_{2\perp})} (u^i + i\partial_x^i/k^+) (u^i - i\partial_y^i/k^+) \\ &\quad \times \frac{1}{N_c^2 - 1} \langle \text{Tr} \mathcal{G}(L^+, \mathbf{z}_{1\perp}; x^+, \mathbf{x}_\perp; k^+) \mathcal{U}_q(x^+, y^+) \mathcal{G}^\dagger(L^+, \mathbf{z}_{2\perp}; y^+, \mathbf{y}_\perp; k^+) \rangle, \end{aligned} \quad (4.1)$$

where $\mathcal{U}_q(x^+, y^+)$ is given by Eq. (3.7) with $\mathbf{r}_\perp(z^+) = \mathbf{u}_\perp z^+$ and it is understood that after the performing the transverse derivatives ∂_x^i and ∂_y^i one sets $\mathbf{x}_\perp = \mathbf{u}_\perp x^+$ and $\mathbf{y}_\perp = \mathbf{u}_\perp y^+$. In writing Eq. (4.1) we have restricted the time integrals to $0 < y^+ < x^+ < L^+$ and multiplied the result by a factor of 2. The Feynman graph representing this emission is shown in Fig. 4.

Note that the quark Wilson lines prior to the first emission time y^+ have canceled each other between the direct and the complex conjugate amplitude. The color trace in the last line

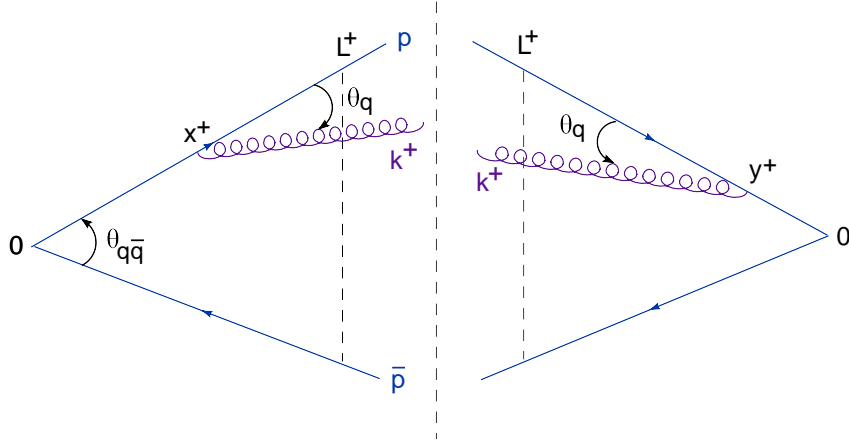


Figure 4: The standard representation of the Feynman graph for direct emission by the quark (amplitude times the complex conjugate amplitude).

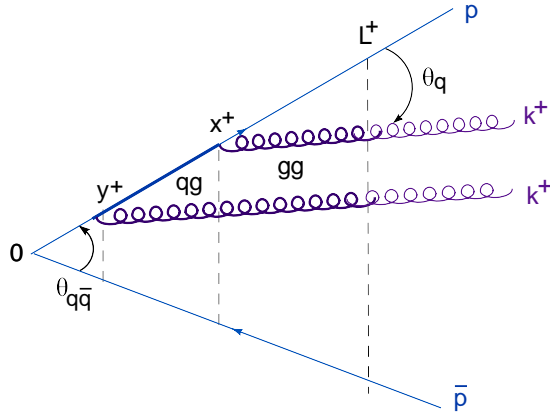


Figure 5: A folded version of the Feynman graph for direct emission where the amplitude and the complex conjugate amplitude are represented on top of each other, to more clearly exhibit the qg and gg dipoles. The (quark and gluon) Wilson lines are indicated with thick lines.

of Eq. (4.1) can be further simplified by using the fact that the background field correlations are local in time. To that aim one first uses the composition law (3.14) to break the last gluon propagator in Eq. (4.1) into two pieces — from y^+ to x^+ and from x^+ to L^+ . Then the medium average factorizes as (below, the k^+ variable is kept implicit, to simplify writing)

$$\begin{aligned}
& \int dz_{\perp} \frac{1}{N_c^2 - 1} \langle \text{Tr} \mathcal{G}(L^+, z_{1\perp}; x^+, \mathbf{x}_{\perp}) \mathcal{U}_q(x^+, y^+) \mathcal{G}^{\dagger}(x^+, z_{\perp}; y^+, \mathbf{y}_{\perp}) \mathcal{G}^{\dagger}(L^+, z_{2\perp}; x^+, z_{\perp}) \rangle \\
&= \int dz_{\perp} \frac{1}{N_c^2 - 1} \langle \text{Tr} \mathcal{G}(L^+, z_{1\perp}; x^+, \mathbf{x}_{\perp}) \mathcal{G}^{\dagger}(L^+, z_{2\perp}; x^+, z_{\perp}) \rangle \\
&\quad \times \frac{1}{N_c^2 - 1} \langle \text{Tr} \mathcal{U}_q(x^+, y^+) \mathcal{G}^{\dagger}(x^+, z_{\perp}; y^+, \mathbf{y}_{\perp}) \rangle. \tag{4.2}
\end{aligned}$$

The two color traces in the r.h.s. of Eq. (4.2) are recognized as the 2-body propagators of two effective dipoles — a quark–gluon (qg) dipole extending from y^+ to x^+ and a gluon–gluon (gg) dipole from x^+ to L^+ — whose interactions in the medium are here computed beyond the eikonal approximation (cf. the discussion after Eq. (3.12)). These dipoles can be easier

visualized by folding the Feynman graph in Fig. 4 in such a way that the direct and complex conjugate amplitudes overlap with each other, as shown in Fig. 5.

Using (3.11), one obtains the following path–integral representation for the propagator of the qg dipole:

$$\begin{aligned} \mathcal{K}_{qg}(x^+, \mathbf{z}_\perp; y^+, \mathbf{y}_\perp; k^+) &\equiv \frac{1}{N_c^2 - 1} \langle \text{Tr} \mathcal{U}_q(x^+, y^+) \mathcal{G}^\dagger(x^+, \mathbf{z}_\perp; y^+, \mathbf{y}_\perp) \rangle \\ &= \int [D\mathbf{r}_\perp] \exp \left\{ -i \frac{k^+}{2} \int_{y^+}^{x^+} dz^+ \dot{\mathbf{r}}_\perp^2 \right\} S_{qg}(x^+, y^+; [\mathbf{r}_\perp - \mathbf{u}_\perp z^+]), \end{aligned} \quad (4.3)$$

which features a qg pair with fluctuating size $\mathbf{r}_\perp(z^+) - \mathbf{u}_\perp z^+$ and path–dependent S –matrix

$$S_{qg}(x^+, y^+; [\mathbf{r}_\perp - \mathbf{u}_\perp z^+]) \simeq \exp \left\{ -\frac{1}{4} \hat{q} \rho \int_{y^+}^{x^+} dz^+ (\mathbf{r}_\perp(z^+) - \mathbf{u}_\perp z^+)^2 \right\}. \quad (4.4)$$

We recall that the boundary conditions for the gluon paths are $\mathbf{r}_\perp(y^+) = \mathbf{y}_\perp$ and $\mathbf{r}_\perp(x^+) = \mathbf{z}_\perp$ and that ρ is a slowly varying function of the dipole size (cf. Eq. (3.26)).

As for the gg dipole in Eq. (4.2), the corresponding mathematics turns out to be simpler: on the average, the medium is homogeneous in the transverse plane, as manifest on Eq. (3.3). Then the medium averaging also averages out the fluctuations in the dipole transverse size, with the net effect that the respective S –matrix depends only upon the *initial* dipole size at time x^+ , that is $\mathbf{x}_\perp - \mathbf{z}_\perp$. Specifically, the following identity holds (see e.g. [19, 32] for details) :

$$\begin{aligned} &\int d\mathbf{z}_{1\perp} \int d\mathbf{z}_{2\perp} e^{-i\mathbf{k}_\perp \cdot (\mathbf{z}_{1\perp} - \mathbf{z}_{2\perp})} \frac{1}{N_c^2 - 1} \langle \text{Tr} \mathcal{G}(L^+, \mathbf{z}_{1\perp}; x^+, \mathbf{x}_\perp) \mathcal{G}^\dagger(L^+, \mathbf{z}_{2\perp}; x^+, \mathbf{z}_\perp) \rangle \\ &= e^{-i\mathbf{k}_\perp \cdot (\mathbf{x}_\perp - \mathbf{z}_\perp)} S_{gg}(L^+, x^+; \mathbf{x}_\perp - \mathbf{z}_\perp), \end{aligned} \quad (4.5)$$

with (compare to Eq. (3.27))

$$S_{gg}(L^+, x^+; \mathbf{x}_\perp - \mathbf{z}_\perp) \simeq \exp \left\{ -\frac{1}{4} \hat{q} \rho(L^+ - x^+) (\mathbf{x}_\perp - \mathbf{z}_\perp)^2 \right\}. \quad (4.6)$$

Note that in writing Eqs. (4.4) and (4.6) above, we have tacitly assumed that the respective dipole sizes are much smaller than μ_D^{-1} , so that the approximations leading to Eqs. (3.26)–(3.27) indeed apply. This will be checked later, when we shall see that the typical dipole sizes are of order $1/k_f$ for (4.4) and respectively of order $1/Q_s$ for (4.6).

Putting together the previous results, we deduce the following expression for the probability for direct emission from the quark

$$\begin{aligned} \mathcal{P}_q^{(\text{in})}(\mathbf{k}) &= 2g^2 C_F \text{Re} \int_0^{L^+} dx^+ \int_0^{x^+} dy^+ e^{ik^+ u^- (x^+ - y^+)} (u^i + i\partial_x^i/k^+) (u^i - i\partial_y^i/k^+) \\ &\quad \times \int d\mathbf{z}_\perp e^{-i\mathbf{k}_\perp \cdot (\mathbf{x}_\perp - \mathbf{z}_\perp)} \mathcal{K}_{qg}(x^+, \mathbf{z}_\perp; y^+, \mathbf{y}_\perp; k^+) S_{gg}(L^+, x^+; \mathbf{x}_\perp - \mathbf{z}_\perp), \end{aligned} \quad (4.7)$$

where it is understood that $\mathbf{x}_\perp \rightarrow \mathbf{u}_\perp x^+$ and $\mathbf{y}_\perp \rightarrow \mathbf{u}_\perp y^+$ after taking the derivatives. Within the limits of our calculation, this expression is exact. It is also rather formal, in the sense of involving a path integral and holding for an arbitrary kinematics of the emitted gluon. In the ‘harmonic approximation’, which consists in treating the slowly varying logarithm ρ in Eqs. (4.4)

and (4.6) as a fixed quantity, the integrations become Gaussian and can be performed exactly (see the Appendix). To keep the discussion as intuitive as possible, in what follows we shall perform a series of approximations which are valid in the kinematics of interest.

But before we proceed with more formal steps, let us emphasize a point of physics⁷: the gluon formation time τ_f for medium-induced radiation is controlled by the intermediate, quark-gluon dipole, stage of the dynamics in Eq. (4.7) and hence it is of the order of the typical duration $x^+ - y^+$ of that stage. Indeed, the S -matrix (4.4) of this *effective* dipole, built with the quark in the direct amplitude and the gluon in the complex conjugate one (or vice-versa), is a measure of the color coherence between the emitted gluon and the parent quark. So long as this dipole is relatively small (meaning for sufficiently small time separations $x^+ - y^+$), one has $S_{qg} \simeq 1$ and then one cannot distinguish the gluon from the quark: in any process involving color exchanges, the emerging quark-gluon pair acts in the same way as the original, bare, quark would do. But with increasing $x^+ - y^+$, the dipole size increases (via gluon diffusion) and then S_{qg} starts to decrease from one, because of the medium rescattering. One can consider the gluon as being formed when the qg dipole suffers a first inelastic collision in the medium, *i.e.* when the exponent in S_{qg} becomes of $\mathcal{O}(1)$. The respective value of $x^+ - y^+$ sets the formation time. For even larger values of x^+ , one has $S_{qg} \ll 1$ and the emission probability is strongly suppressed.

The starting point of our approximation is an expression for the propagator (4.3) of the qg dipole valid in the harmonic approximation. With $\rho \approx \text{const.}$ and absorbed into the normalization of \hat{q} for convenience⁸, the path integral (4.3) describes a harmonic oscillator with *imaginary squared frequency*

$$\Omega^2 = i \frac{\hat{q}}{2k^+} \implies \Omega = \frac{1+i}{\sqrt{2}} \sqrt{\frac{\hat{q}}{2k^+}}, \quad (4.8)$$

and hence it can be exactly computed (see e.g. [11, 19] for details and also the Appendix below). To be specific, let us ignore the transverse derivatives in Eq. (4.7) for the time being (we shall return to them latter) and fix $\mathbf{x}_\perp = \mathbf{u}_\perp x^+$ and $\mathbf{y}_\perp = \mathbf{u}_\perp y^+$. Then one obtains

$$\begin{aligned} \mathcal{K}_{qg}(x^+, \mathbf{b}_\perp + \mathbf{u}_\perp x^+; y^+, \mathbf{u}_\perp y^+; k^+) &= \exp \left\{ -ik^+ \left[(x^+ - y^+) \frac{\mathbf{u}_\perp^2}{2} + \mathbf{u}_\perp \cdot \mathbf{b}_\perp \right] \right\} \\ &\times \mathcal{K}_{qg}(x^+, \mathbf{b}_\perp; y^+, \mathbf{0}_\perp; k^+) \end{aligned} \quad (4.9)$$

where we set $\mathbf{b}_\perp \equiv \mathbf{z}_\perp - \mathbf{u}_\perp x^+$ and

$$\mathcal{K}_{qg}(x^+, \mathbf{b}_\perp; y^+, \mathbf{0}_\perp; k^+) = \frac{k^+ \Omega}{2\pi i \sinh \Omega(x^+ - y^+)} \exp \left\{ -\frac{k^+ \Omega}{2i} \coth \Omega(x^+ - y^+) \mathbf{b}_\perp^2 \right\}. \quad (4.10)$$

The quantity \mathbf{b}_\perp is the transverse size of the qg dipole at time x^+ and thus also the size of the ensuing gg dipole at any time $z^+ > x^+$. We shall denote

$$\tau_f \equiv \frac{1}{|\Omega|} = \sqrt{\frac{2k^+}{\hat{q}}}, \quad (4.11)$$

⁷We would like to thank Al Mueller for an illuminating discussion of this point.

⁸This is a standard convention in the literature; the factors of ρ can be recovered, if needed, by replacing everywhere $\hat{q} \rightarrow \hat{q}\rho$.

anticipating that this quantity plays the role of the formation time.

Two limits of Eq. (4.10) will be useful in what follows:

(i) *Small times* $|\Omega|(x^+ - y^+) \ll 1$ or $x^+ - y^+ \ll \tau_f$: then, by expanding the r.h.s. of Eq. (4.10) to quadratic order in $|\Omega|(x^+ - y^+)$ one finds

$$\mathcal{K}_{qg}(x^+, \mathbf{b}_\perp; y^+, \mathbf{0}_\perp; k^+) \simeq \frac{k^+}{2\pi i(x^+ - y^+)} \exp \left\{ -i \frac{k^+ b_\perp^2}{2(x^+ - y^+)} - \frac{1}{12} \hat{q} (x^+ - y^+) b_\perp^2 \right\}. \quad (4.12)$$

This is recognized as the saddle point approximation to (4.3) with the saddle point determined by the kinetic piece of the action alone; that is, $\mathcal{K}_{qg} \approx \mathcal{G}_0 S_{qg}$ where \mathcal{G}_0 is the free propagator (3.12) and S_{qg} is the S -matrix (4.4) evaluated along the classical path, which reads :

$$\mathbf{r}_{\text{class}}(z^+) - \mathbf{u}_\perp z^+ = \frac{z^+ - y^+}{x^+ - y^+} \mathbf{b}_\perp. \quad (4.13)$$

(ii) *Large times* $|\Omega|(x^+ - y^+) \gg 1$ or $x^+ - y^+ \gg \tau_f$: then, one finds

$$\mathcal{K}_{qg}(x^+, \mathbf{b}_\perp; y^+, \mathbf{0}_\perp; k^+) \propto \frac{k^+}{\tau_f} e^{-(x^+ - y^+)/\tau_f} \exp \left\{ -\frac{1+i}{4} \sqrt{\hat{q} k^+} b_\perp^2 \right\}. \quad (4.14)$$

Eq. (4.12) implies that, at early times $x^+ - y^+ \lesssim \tau_f$, the size of the qg dipole increases through diffusion, $b_\perp^2 \propto (x^+ - y^+)/k^+$ (as shown by the first term in the exponent) and this increase enhances the dipole rescattering off the medium (as described by the second term in the exponent of Eq. (4.12), coming from S_{qg}). When $x^+ - y^+ \simeq \tau_f$, this second term becomes of order one, showing that τ_f is the formation time, as anticipated. For larger times $x^+ - y^+ \gg \tau_f$, the dipole propagator is exponentially suppressed, cf. Eq. (4.14), meaning that the color coherence of the qg pair has been destroyed by the medium. The maximal size of the qg dipole, as attained for $x^+ - y^+ \simeq \tau_f$, is⁹

$$b_f^2 \simeq \frac{\tau_f}{k^+} \sim \frac{1}{\sqrt{\hat{q}\omega}}. \quad (4.15)$$

Via the uncertainty principle, this yields the typical transverse momentum of the gluon at the formation time as $k_f^2 \simeq 1/b_f^2 \simeq \sqrt{\omega\hat{q}}$, in agreement with Eq. (2.4). This obeys the scaling law $k_f^2 \simeq \hat{q}\tau_f$ showing that this transverse momentum has been acquired via medium rescattering during a time τ_f . Since $\tau_f \ll L^+$, this k_\perp is much smaller than the final momentum of the gluon, which can be as large as $k_\perp \sim Q_s$, as we shall shortly see.

To compute the final gluon spectrum, one has to also take into account the medium rescattering *after* the time of formation, as encoded in the S -matrix (4.6) of the gg dipole. Specifically, the function $S_{gg}(L^+, x^+; \mathbf{x}_\perp - \mathbf{z}_\perp)$ controls the range of the integration over $\mathbf{z}_\perp = \mathbf{b}_\perp + \mathbf{u}_\perp x^+$, which in turn fixes the final transverse momentum \mathbf{k}_\perp via the Fourier transform in Eq. (4.7). As we shall shortly check, the typical values for b_\perp allowed by the gg dipole are much smaller than b_f . Hence, in evaluating this Fourier transform, one can replace the propagator \mathcal{K}_{qg} of the qg dipole by the corresponding free propagator \mathcal{G}_0 (which carries the whole dependence upon \mathbf{b}_\perp in the limit where $b_\perp \ll b_f$). Then the integral over \mathbf{b}_\perp reduces to

$$e^{-i \frac{k^+ \mathbf{u}_\perp^2}{2} (x^+ - y^+)} \int d\mathbf{b}_\perp e^{i \mathbf{b}_\perp \cdot (\mathbf{k}_\perp - k^+ \mathbf{u}_\perp)} \exp \left\{ \frac{-i k^+ b_\perp^2}{2(x^+ - y^+)} \right\} \exp \left\{ -\frac{\hat{q}}{4} (L^+ - x^+) b_\perp^2 \right\}, \quad (4.16)$$

⁹As usual, when writing parametric estimates, we ignore numerical factors and identify k^+ with ω .

where it was important to also include the phase factor in the r.h.s. of Eq. (4.9) (which is a part of the free propagator $\mathcal{G}_0(x^+, \mathbf{b}_\perp + \mathbf{u}_\perp x^+; y^+, \mathbf{u}_\perp y^+; k^+)$). The overall phase in front of the above integral is such that it exactly cancels the phase $e^{ik^+ u^-(x^+ - y^+)}$ in Eq. (4.7). This is worth emphasizing in view of the discussion of the interference terms in Sect. 5, where the corresponding phase cancellation does *not* hold — which in turn has important consequences.

For medium-induced radiation, the time variables x^+ and y^+ can lie anywhere within the medium, $0 < x^+, y^+ < L^+$ (except very close to the boundaries¹⁰), so long as $x^+ - y^+ \sim \tau_f \ll L^+$. Accordingly $\hat{q}(L^+ - x^+) \sim \hat{q}L^+ = Q_s^2$ is much larger than $k^+/\tau_f \sim k_f^2$ (recall Eq. (2.4)), so the integral in Eq. (4.16) is controlled by the last factor inside the integrand and yields

$$\int d\mathbf{b}_\perp e^{i\mathbf{b}_\perp \cdot (\mathbf{k}_\perp - k^+ \mathbf{u}_\perp)} \exp\left\{-\frac{1}{4} Q_s^2 b_\perp^2\right\} \sim \frac{1}{Q_s^2} \exp\left\{-\frac{(\mathbf{k}_\perp - k^+ \mathbf{u}_\perp)^2}{Q_s^2}\right\}. \quad (4.17)$$

Note that $k^+ \mathbf{u}_\perp$ is the transverse momentum inherited by the gluon from its parent quark. Accordingly, $\mathbf{k}_\perp - k^+ \mathbf{u}_\perp$ is the additional transverse momentum acquired by the gluon from the medium and is the same as the component of the gluon momentum which is transverse to the quark; indeed, using Eq. (3.22) one can write

$$(\mathbf{k}_\perp - k^+ \mathbf{u}_\perp)^2 = 2k^+(k \cdot u) \simeq (\omega\theta_q)^2. \quad (4.18)$$

Hence, Eq. (4.17) shows that the momentum gained by the gluon via medium rescattering can be as large as Q_s , as anticipated. Since $Q_s \gg k_f$, it is clear that most of this momentum gets accumulated *after* the gluon formation (as also shown by the fact that the integral (4.17) is controlled by the S -matrix of the final gg dipole).

The last ingredient that we need in order to evaluate Eq. (4.7) is the action of the transverse derivatives like $(u^i + i\partial_x^i/k^+)$. These will be shortly computed, but their effect can be anticipated on physical grounds: from the construction of the amplitude in Eq. (3.17), we recall that the derivative ∂_x^i acts on the gluon propagator at the emission point. Hence, the operator $(u^i + i\partial_x^i/k^+)$ measures the difference between the transverse orientations of the source and of the emitted gluon, at the time of formation. Then, clearly, we expect its magnitude to be of order $\theta_f \equiv k_f/\omega$ (the formation angle introduced in Eq. (2.6)). To explicitly check that, one needs to compute

$$(u^i + i\partial_x^i/k^+)(u^i - i\partial_y^i/k^+) \mathcal{K}_{qg}(x^+, \mathbf{b}_\perp + \mathbf{x}_\perp; y^+, \mathbf{y}_\perp; k^+) \quad (4.19)$$

with the derivatives evaluated at $\mathbf{x}_\perp = \mathbf{u}_\perp x^+$ and $\mathbf{y}_\perp = \mathbf{u}_\perp y^+$. The general expression for \mathcal{K}_{qg} which is required for that purpose is given in the Appendix. But for a parametric estimate, one can replace \mathcal{K}_{qg} by the free propagator \mathcal{G}_0 . We thus deduce

$$\begin{aligned} \left(u^i - \frac{i\partial_y^i}{k^+}\right) \left(u^i + \frac{i\partial_x^i}{k^+}\right) \mathcal{G}_0 &= \left(u^i - \frac{i\partial_y^i}{k^+}\right) \left[\left(u^i - k^+ \frac{b^i + x^i - y^i}{x^+ - y^+}\right) \mathcal{G}_0 \right] \\ &= \left[\frac{b_\perp^2}{(x^+ - y^+)^2} + \frac{2i}{k^+(x^+ - y^+)} \right] \mathcal{G}_0 \end{aligned} \quad (4.20)$$

¹⁰Very small values $0 < x^+, y^+ < \omega/Q_s^2 \ll \tau_f$ corresponds to vacuum-like emissions with relatively large momenta $k_\perp \gtrsim Q_s$. Values close to L^+ , such that $L^+ - \tau_f < x^+, y^+ < L^+$, yield boundary terms which cancel when summing up together the (in, in), (in, out), and (out, out) contributions.

where the last equality is obtained after setting $x^i - y^i = u^i(x^+ - y^+)$. Using $x^+ - y^+ \sim \tau_f$ and $b_\perp \sim 1/Q_s$, it is easy to check that the second term in the square brackets is the dominant one and is of order $1/(k^+\tau_f) \sim \theta_f^2$, as anticipated.

We are finally in a position to estimate the spectrum (4.7) for direct emissions. To that aim, one has to multiply the Gaussian in Eq. (4.17) by a factor $L^+\tau_f$ coming from the integrals over the time variables y^+ and x^+ (this factor is the longitudinal phase-space for medium-induced gluon radiation), by the factor θ_f^2 which estimates the effects of the transverse derivatives, by a factor $k^+/(x^+ - y^+) \sim \omega/\tau_f$ coming from the normalization of \mathcal{G}_0 in Eq. (4.12) and, finally, by the overall factor g^2C_F manifest on Eq. (4.7). Putting all that together, one finds

$$\mathcal{P}_q^{(\text{in})}(\omega, \mathbf{k}_\perp) \propto \alpha_s C_F \theta_f^2 L^+ \frac{\omega}{Q_s^2} \exp\left\{-\frac{(\mathbf{k}_\perp - k^+ \mathbf{u}_\perp)^2}{Q_s^2}\right\}. \quad (4.21)$$

Eq. (4.21) is indeed the expected parametric estimate for the BDMPS-Z spectrum of the medium-induced radiation by a quark. A perhaps more familiar form of this spectrum is obtained by using Eq. (2.6) for θ_f to deduce (for $\mathbf{u}_\perp = 0$)

$$\omega \frac{dN}{d\omega dk_\perp^2} \propto \frac{\alpha_s C_F}{\sqrt{\omega \hat{q}}} \exp\left\{-\frac{k_\perp^2}{Q_s^2}\right\}. \quad (4.22)$$

It is here understood that $k_\perp \gtrsim k_f \simeq (\omega \hat{q})^{1/4}$, since the gluon acquires a transverse momentum of order k_f already by the time of formation. The spectrum (4.22) is roughly flat in the range $k_f < k_\perp < Q_s$ and it is exponentially suppressed at larger values $k_\perp \gg Q_s$. After integration over k_\perp and recalling that $Q_s^2 = \hat{q}L^+ \gg k_f^2$ and $\omega_c = \hat{q}L^2/2$, this yields

$$\omega \frac{dN}{d\omega} \propto \alpha_s C_F \sqrt{\frac{\omega_c}{\omega}} \implies \Delta E \equiv \int_0^{\omega_c} \omega \frac{dN}{d\omega} \propto \alpha_s C_F \omega_c, \quad (4.23)$$

where the integration has been restricted to the phase-space for medium-induced radiation, *i.e.* $\hat{q}^{1/3} < \omega \leq \omega_c$, cf. Eq. (2.8) (but the lower limit is irrelevant for computing the total energy loss, which is dominated by the upper limit ω_c).

It is finally interesting to compare the spectrum (4.22) for medium-induced radiation to the bremsstrahlung spectrum in Eq. (2.2), for the same kinematics. By inspection of these equations, it is apparent that the medium-induced spectrum is formally the same (for any k_\perp within the range $k_f < k_\perp < Q_s$) as the vacuum spectrum evaluated at $k_\perp = k_f$. Hence, clearly,

$$\frac{\mathcal{P}_q^{(\text{in})}}{\mathcal{P}_q^{(\text{vac})}} \sim \frac{k_\perp^2}{\sqrt{\omega \hat{q}}} \sim \frac{k_\perp^2}{k_f^2}, \quad (4.24)$$

which shows that the medium-induced radiation dominates over bremsstrahlung for all the relevant momenta. This ratio is largest for $k_\perp \simeq Q_s$, when it becomes

$$\frac{\mathcal{P}_q^{(\text{in})}}{\mathcal{P}_q^{(\text{vac})}} \sim \frac{L^+}{\tau_f} \sim \sqrt{\frac{\omega_c}{\omega}} \gg 1 \quad \text{for } k_\perp \simeq Q_s. \quad (4.25)$$

Physically, this is so because a gluon which is formed via medium rescattering can be emitted at any place inside the medium ($x^+, y^+ \lesssim L^+$), in contrast to the vacuum-like emissions, which are restricted to relatively short distances/times $x^+, y^+ \lesssim \tau_q \ll L^+$. Accordingly, the longitudinal phase-space $L^+\tau_f$ for medium-induced radiation is parametrically larger than the corresponding phase-space $\sim \tau_q^2$ for bremsstrahlung.

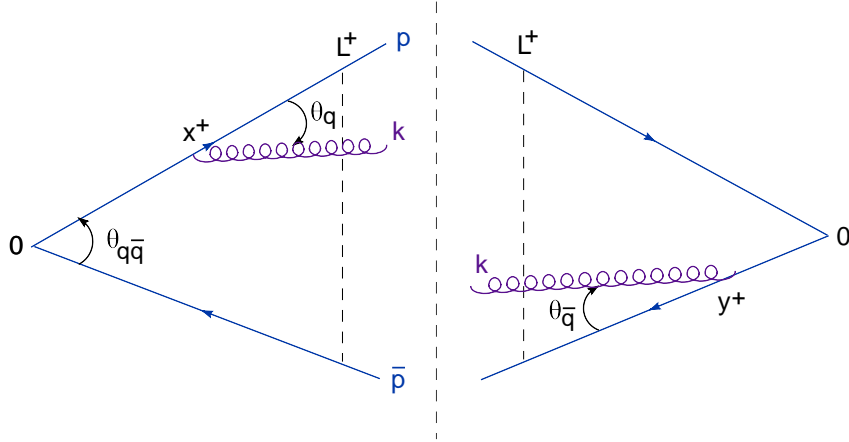


Figure 6: A Feynman graph for interference (amplitude times the complex conjugate amplitude).

5. Medium-induced gluon radiation: interference terms

We now turn to the main problem of interest for us in this paper, namely the contribution of the quark–antiquark interference to the medium–induced gluon radiation (see Fig. 6). Once again, we shall focus on the (in, in) piece, where the gluons are emitted inside the medium in both the direct and the complex conjugate amplitude. The respective contribution to the gluon spectrum is obtained by multiplying the quark amplitude (3.17) by the complex conjugate of the corresponding antiquark amplitude, performing the average over the medium and the sum (average) over the final (initial) color indices. This yields

$$\begin{aligned}
\mathcal{I}^{(\text{in})}(\mathbf{k}) &= -2g^2 C_F \operatorname{Re} \int_0^{L^+} dx^+ \int_0^{x^+} dy^+ e^{ik^+(u^- x^+ - \bar{u}^- y^+)} \\
&\quad \times \int dz_{1\perp} \int dz_{2\perp} e^{-i\mathbf{k}_\perp \cdot (\mathbf{z}_{1\perp} - \mathbf{z}_{2\perp})} (u^i + i\partial_x^i/k^+) (\bar{u}^i - i\partial_y^i/k^+) \\
&\quad \times \frac{1}{N_c^2 - 1} \langle \operatorname{Tr} \mathcal{G}(L^+, \mathbf{z}_{1\perp}; x^+, \mathbf{x}_\perp; k^+) \mathcal{U}_q(x^+, 0) \mathcal{U}_{\bar{q}}^\dagger(y^+, 0) \mathcal{G}^\dagger(L^+, \mathbf{z}_{2\perp}; y^+, \mathbf{y}_\perp; k^+) \rangle, \\
&\quad + (q \rightarrow \bar{q}),
\end{aligned} \tag{5.1}$$

where the Wilson lines $\mathcal{U}_q(x^+, 0)$ and $\mathcal{U}_{\bar{q}}^\dagger(y^+, 0)$ refer to the quark and the antiquark, respectively, and it is understood that after performing the transverse derivatives ∂_x^i and ∂_y^i one has to identify \mathbf{x}_\perp and \mathbf{y}_\perp with the emission points $\mathbf{u}_\perp x^+$ and $\bar{\mathbf{u}}_\perp y^+$, respectively. The explicit integrals in Eq. (5.1) are written for the situation where the gluon is emitted at x^+ by the quark in the direct amplitude and absorbed by the antiquark at y^+ in the complex conjugate amplitude, with $y^+ < x^+$. The other possible configurations are obtained by exchanging the quark and the antiquark, as indicated in the last line of Eq. (5.1). After ‘folding’ the Feynman graph as shown in Fig. 7, in such a way to superpose direct and conjugate amplitudes, one can view y^+ as the ‘first emission time’, for an emission off the antiquark, and x^+ as the ‘second emission time’, for an emission by the quark. Although somewhat formal, this perspective allows one to easily visualise the effective ‘color dipoles’ encoded in Eq. (5.1), that we now discuss.

The subsequent manipulations are rather similar to those in Sect. 4. Once again, one splits the quark Wilson line as $\mathcal{U}_q(x^+, 0) = \mathcal{U}_q(x^+, y^+) \mathcal{U}_q(y^+, 0)$ and one breaks the last gluon propa-

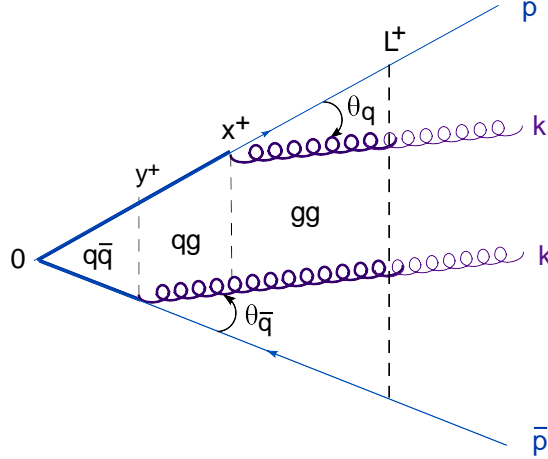


Figure 7: A folded version of the Feynman graph for interference where the amplitude and the complex conjugate amplitude are represented on top of each other, to more clearly exhibit the $q\bar{q}$, qg and gg dipoles. The (quark and gluon) Wilson lines are indicated with thick lines.

gator into two pieces — from y^+ to x^+ and from x^+ to L^+ —, by introducing an intermediate integration point z_\perp . Then one uses the locality of the medium correlations in time to factorize the color trace into effective dipole contributions (cf. Eq. (4.2)). This procedure now generates three dipole S -matrices: a quark–antiquark ($q\bar{q}$) dipole which extends in time from 0 up to y^+ , a quark–gluon (qg) dipole from y^+ to x^+ , and a gluon–gluon (gg) dipole from x^+ to L^+ . The integrations over $z_{1\perp}$ and $z_{2\perp}$ are again performed as in Eq. (4.5) and the outcome can be written as (compare to Eq. (4.7))

$$\begin{aligned} \mathcal{I}^{(\text{in})}(\mathbf{k}) &= -2g^2 C_F \text{Re} \int_0^{L^+} dx^+ \int_0^{x^+} dy^+ e^{ik^+(u^-x^+ - \bar{u}^-y^+)} (u^i + i\partial_x^i/k^+) (\bar{u}^i - i\partial_y^i/k^+) \\ &\quad \times S_{q\bar{q}}(y^+, 0) \int dz_\perp e^{-ik_\perp \cdot (x_\perp - z_\perp)} \mathcal{K}_{qg}(x^+, z_\perp; y^+, \mathbf{y}_\perp; k^+) S_{gg}(L^+, x^+; \mathbf{x}_\perp - z_\perp) \\ &\quad + (q \rightarrow \bar{q}), \end{aligned} \quad (5.2)$$

where it is understood that $\mathbf{x}_\perp \rightarrow \mathbf{u}_\perp x^+$ and $\mathbf{y}_\perp \rightarrow \bar{\mathbf{u}}_\perp y^+$ after taking the derivatives. The $q\bar{q}$ dipole is evaluated similarly to Eq. (3.29) :

$$S_{q\bar{q}}(y^+, 0) \simeq \exp\left\{-\frac{1}{12} \hat{q} \rho (\mathbf{u}_\perp - \bar{\mathbf{u}}_\perp)^2 (y^+)^3\right\} \simeq \exp\left\{-\frac{1}{24} \hat{q} \theta_{q\bar{q}}^2 (y^+)^3 \rho\right\}. \quad (5.3)$$

(We have also used $(\mathbf{u}_\perp - \bar{\mathbf{u}}_\perp)^2 \simeq \theta_{q\bar{q}}^2/2$ for small angles.) The qg dipole is now built with the *quark* line in the direct amplitude and the gluon emitted by the *antiquark* in the complex conjugate amplitude. The corresponding propagator \mathcal{K}_{qg} is defined as in Eqs. (4.3)–(4.4) but with different boundary conditions for the path integral (4.3), namely $\mathbf{r}_\perp(y^+) = \bar{\mathbf{u}}_\perp y^+$ and $\mathbf{r}_\perp(x^+) = z_\perp$. Finally, the gg dipole is given by Eq. (4.6), as before.

There are several important differences between the interference term (5.2) and the corresponding expression (4.7) for the direct emission. Two of them are quite obvious:

(a) The presence of the initial $q\bar{q}$ dipole, which measures the *color coherence* between the quark and the antiquark at the time y^+ of the first emission, which is restricted to

$$y^+ \lesssim \tau_{coh} \simeq \left(\frac{24}{\hat{q}\rho\theta_{q\bar{q}}^2} \right)^{1/3} \sim L^+ \left(\frac{\theta_c}{\theta_{q\bar{q}}} \right)^{2/3}. \quad (5.4)$$

For larger values $y^+ \gtrsim \tau_{coh}$, one has $S_{q\bar{q}}(y^+, 0) \ll 1$, that is, the color coherence is washed out. The parametric estimate in the r.h.s. shows that $\tau_{coh} \ll L^+$ so long as $\theta_{q\bar{q}} \gg \theta_c$. (As before, in writing parametric estimates we neglect numerical factors and treat ρ as a constant of $\mathcal{O}(1)$.)

(b) The fact that the qg dipole starts at y^+ with a non-zero transverse size r_0 equal to the separation between the quark and the antiquark at that time (the maximal size of the $q\bar{q}$ dipole): $r_0 = |\mathbf{u}_\perp - \bar{\mathbf{u}}_\perp|y^+ \sim \theta_{q\bar{q}}y^+$.

A third difference between direct and interference terms, which is perhaps less obvious at this stage but will play a major role for the final results, is the following:

(c) The vacuum-like phase $e^{ik^+(u^-x^+ - \bar{u}^-y^+)}$ in Eq. (5.2) is not compensated in the calculation of medium-induced radiation, in contrast to what happened for the direct emissions (recall the discussion after Eq. (4.16)). Rather, there is a left-over phase which controls the *quantum coherence* between the two emitters (see Eq. (5.10) below).

By itself, the constraint (5.4) represents a strong limitation on the longitudinal phase-space for interference and shows that the interference terms are suppressed with respect to the direct emissions. However, it turns out that the limitation introduced by the quantum coherence, cf. point (c) above, can be even stronger, depending upon the value of $\theta_{q\bar{q}}$. To understand the interplay between the different types of coherence, we shall now perform a more detailed analysis of Eq. (5.2).

The first step consists in clarifying the formation time. From Sect. 4, we recall that this is controlled by the propagator \mathcal{K}_{qg} of the quark-gluon dipole. In the present case, this propagator measures the (quantum and color) coherence between the gluon emitted by one of the emitters and the *other* emitter. The ‘exact’ expression of \mathcal{K}_{qg} valid in the harmonic approximation will be given in the Appendix. Here we shall merely use a combination of small-time and large-time approximations, like in Eqs. (4.12)–(4.14). The time scale separating between the two regimes is, once again, $\tau_f = 1/|\Omega|$, cf. Eq. (4.11).

For small $x^+ - y^+ \ll \tau_f$, \mathcal{K}_{qg} can be approximated by the saddle point approximation to the path integral in Eq. (4.3), with the saddle point determined by the kinetic term alone. The corresponding classical path is readily determined as

$$\mathbf{r}_{\text{class}}(z^+) - \mathbf{u}_\perp z^+ = \mathbf{r}_0 + \frac{z^+ - y^+}{x^+ - y^+} (\mathbf{z}_\perp - \mathbf{u}_\perp x^+ + \mathbf{r}_0), \quad \mathbf{r}_0 \equiv (\bar{\mathbf{u}}_\perp - \mathbf{u}_\perp)y^+. \quad (5.5)$$

As in Sect. 4, it is convenient to change variables from \mathbf{z}_\perp (the gluon transverse position at time x^+) to $\mathbf{b}_\perp \equiv \mathbf{z}_\perp - \mathbf{u}_\perp x^+$ (the final size of the qg dipole and hence also the size of the gg dipole at any time $z^+ \geq x^+$). Then the saddle point (5.5) yields $\mathcal{K}_{qg} \approx \mathcal{G}_0 S_{qg}$, with

$$\mathcal{G}_0(x^+, \mathbf{z}_\perp; y^+, \bar{\mathbf{u}}_\perp y^+; k^+) = \frac{k^+}{2\pi i(x^+ - y^+)} \exp \left\{ -i \frac{k^+(\mathbf{b}_\perp + \mathbf{u}_\perp x^+ - \bar{\mathbf{u}}_\perp y^+)^2}{2(x^+ - y^+)} \right\}, \quad (5.6)$$

$$S_{qg}(x^+, y^+; \mathbf{b}_\perp) \approx \exp \left\{ -\frac{1}{12} \hat{q}(x^+ - y^+)(b_\perp^2 + r_0^2 + \mathbf{b}_\perp \cdot \mathbf{r}_0) \right\}. \quad (5.7)$$

For larger time difference, $x^+ - y^+ \gg \tau_f$, the qg dipole is exponentially suppressed, as manifest on Eq. (4.14) : $\mathcal{K}_{qg} \propto e^{-(x^+ - y^+)/\tau_f}$.

So, clearly, the actual formation time cannot be larger than τ_f . However, depending upon the value of $r_0 \sim \theta_{q\bar{q}} y^+$, this time could be *shorter* — that would be the case if the exponent in Eq. (5.7) could become of order one already for $x^+ - y^+ \ll \tau_f$. To find out what is the actual scenario, one needs to consider \mathcal{K}_{qg} simultaneously with the other constraints on the time integrations in Eq. (5.2), which are specific to the interference problem. The first one is the condition for color coherence between the two emitters, as expressed by Eq. (5.4). The second one is the condition for their quantum coherence, as encoded in the phase $e^{ik^+(u^- x^+ - \bar{u}^- y^+)}$ manifest in Eq. (5.2) together with a similar phase encoded in \mathcal{K}_{qg} .

To better appreciate the role of these phases, let us first consider the vacuum limit of the present calculation. In the vacuum, all the dipole S -matrices are set to one, the function \mathcal{K}_{qg} reduces to the free gluon propagator \mathcal{G}_0 , and then the integral over \mathbf{z}_\perp in Eq. (5.2) is straightforward. Using the integration variable $\mathbf{b}_\perp \equiv \mathbf{z}_\perp - \mathbf{u}_\perp x^+$, one finds

$$e^{ik^+(u^- x^+ - \bar{u}^- y^+)} \int d\mathbf{b}_\perp e^{i\mathbf{b}_\perp \cdot \mathbf{k}_\perp} \mathcal{G}_0(x^+ - y^+; \mathbf{b}_\perp + \mathbf{u}_\perp x^+ - \bar{\mathbf{u}}_\perp y^+) = e^{i(k \cdot u)x^+ - i(k \cdot \bar{u})y^+} \quad (5.8)$$

where the r.h.s. is recognized as the product of phases controlling the in-vacuum emission times, from the quark and the antiquark. These phases imply $x^+ \lesssim \tau_q$ and $y^+ \lesssim \tau_{\bar{q}}$, where we recall that $\tau_q = 1/(k \cdot u) \sim 1/\omega\theta_q^2$ and similarly for $\tau_{\bar{q}}$. Then the time integrations generate the expected longitudinal phase-space $\tau_q \tau_{\bar{q}}$ for interference in the vacuum.

In the case of the medium, the integral over \mathbf{b}_\perp is controlled by the S -matrix $S_{gg}(L^+, x^+; \mathbf{b}_\perp)$ of the gg dipole, which enforces a rather small value $b_\perp \sim 1/Q_s$. (A similar argument applied to direct emissions; recall the discussion after Eq. (4.16).) For such small values of b_\perp , we can replace $\mathcal{K}_{qg} \approx \mathcal{G}_0$ for the purposes of the \mathbf{b}_\perp -integration, which then reduces to

$$e^{ik^+(u^- x^+ - \bar{u}^- y^+)} \int d\mathbf{b}_\perp e^{i\mathbf{b}_\perp \cdot \mathbf{k}_\perp} \exp\left\{-i \frac{k^+(\mathbf{b}_\perp + \mathbf{u}_\perp x^+ - \bar{\mathbf{u}}_\perp y^+)^2}{2(x^+ - y^+)}\right\} \exp\left\{-\frac{1}{4} Q_s^2 b_\perp^2\right\} \\ \sim e^{i\Phi} \frac{1}{Q_s^2} \exp\left\{-\frac{1}{Q_s^2} \left(\mathbf{k}_\perp - k^+ \frac{\mathbf{u}_\perp x^+ - \bar{\mathbf{u}}_\perp y^+}{x^+ - y^+}\right)^2\right\}, \quad (5.9)$$

with the phase

$$\Phi \equiv k^+(u^- x^+ - \bar{u}^- y^+) - \frac{k^+(\mathbf{u}_\perp x^+ - \bar{\mathbf{u}}_\perp y^+)^2}{2(x^+ - y^+)} = -\frac{k^+(\mathbf{u}_\perp - \bar{\mathbf{u}}_\perp)^2 x^+ y^+}{2(x^+ - y^+)}. \quad (5.10)$$

In these manipulations, we have anticipated that $k^+/(x^+ - y^+) \sim k_f^2 \ll Q_s^2$ and we have used $\mathbf{u}_\perp^2 = 2u^-$. At this point, one should recall that in the corresponding calculation for the direct emission, Eqs. (4.16)–(4.17), the analog of this phase Φ has exactly canceled. The phase (5.10) is not quite the same as it would be in the vacuum, cf. Eq. (5.8) : it does not constrain the x^+ and y^+ variables *individually*, but a particular combination of them.

To summarize, the integrations over x^+ and y^+ are controlled by the following product

$$\exp\left\{-i \frac{k^+ \theta_{q\bar{q}}^2 x^+ y^+}{4(x^+ - y^+)}\right\} \exp\left\{-\frac{1}{24} \hat{q}(x^+ - y^+) (\theta_{q\bar{q}} y^+)^2\right\} \exp\left\{-\frac{x^+ - y^+}{\tau_f}\right\}, \quad (5.11)$$

together with the constraint (5.4) coming from color coherence. The first factor in Eq. (5.11) is the ‘vacuum-like’ phase Φ . The second factor comes from the S -matrix (5.7) of the qg dipole, where we have neglected $b_\perp \sim 1/Q_s$ next to $r_0 \sim \theta_{q\bar{q}}y^+$. The third factor is of course the large-time decay of the qg propagator.

The four constraints introduced by the three factors in Eq. (5.11) together with Eq. (5.4) have to be simultaneously considered. Their analysis becomes streamlined if one first identifies the characteristic times scales associated with each of them. Let us enumerate these scales here (they have already appeared in the qualitative discussion in Sect. 2.2):

(i) *the color coherence time* τ_{coh} : this is the maximal value of the first emission time y^+ at which the quark and the antiquark do still form a color singlet. This scale has been already shown in Eq. (5.4);

(ii) *the in-medium formation time* (here in the context of interference) : this is the typical time interval $x^+ - y^+$ during which the qg dipole loses quantum and color coherence. As we shall shortly argue, this scale is still determined by the last factor in Eq. (5.11), like for direct emissions, and thus is equal to τ_f , cf. Eq. (2.4).

(iii) *the transverse resolution time* τ_λ : this represents the characteristic time scale for quantum coherence between the two emitters during the process of gluon formation. This scale is determined by the phase in the first factor in Eq. (5.11): the condition $\Phi \lesssim 1$ together with the fact that $x^+ - y^+ \sim \tau_f$ implies the following constraint on the emission times x^+ and y^+ :

$$x^+y^+ \lesssim \frac{4\tau_f}{k^+\theta_{q\bar{q}}^2} \implies \sqrt{x^+y^+} \lesssim \frac{\lambda_f}{\theta_{q\bar{q}}} \equiv \tau_\lambda, \quad (5.12)$$

where $\lambda_f = 1/k_f$ is the transverse wavelength of the gluon at the time of formation (we have used $\tau_f \sim k^+/k_f^2$). Some useful estimates for τ_λ have been given in Eq. (2.13).

Eq. (5.12) represents in an average way the condition that the gluon overlap with both sources during the formation time. Since $x^+ \simeq y^+ + \tau_f$, it is clear that this condition must be viewed as a constraint on the first emission time y^+ .

(iv) *the interference time* τ_{int} : as discussed in Sect. 2.2, this is the upper limit on y^+ which follows from Eq. (5.12) in the large angle regime where $\theta_{q\bar{q}} \gg \theta_f$ (and hence $\tau_\lambda \ll \tau_f$) :

$$y^+ \lesssim \tau_{int} \equiv \frac{\tau_\lambda^2}{\tau_f} = \frac{2}{\omega\theta_{q\bar{q}}^2}. \quad (5.13)$$

Some useful estimates for τ_{int} are shown in Eq. (5.13). In the other interesting regime at small angles $\theta_{q\bar{q}} \ll \theta_f$ (or $\tau_\lambda \gg \tau_f$), the upper limit on y^+ is essentially τ_λ (see Sect. 2.2 for details).

So far, we have not discussed the time scale introduced by the original size $r_0 \sim \theta_{q\bar{q}}y^+$ of the qg dipole. Moreover, we have implicitly assumed this scale not to influence the formation time. Let us check that this is indeed the case. The exponent in the middle factor in Eq. (5.11) becomes of order one when $x^+ - y^+ \sim \tau_f$ and $y^+ \sim \tau_\lambda$ (we have used $\hat{q}\tau_f \simeq k_f^2$, cf. Eq. (2.4)). This shows that the characteristic time scale associated with r_0 is the same as the scale τ_λ for quantum coherence. Since y^+ cannot become larger than τ_λ , as clear from Eq. (5.12), we conclude that the original dipole size r_0 plays at most a marginal role in the formation process and thus it cannot modify the formation time to parametric accuracy.

We have thus recognized in our calculation all the characteristic time scales for color and quantum coherence that were previously introduced, via physical considerations, in Sect. 2.2.

The interplay between these scales leads to the various regimes for interference identified in Sect. 2.2, that we shall not repeat here. Rather, we shall now explicitly check the arguments in Sect. 2.2 concerning the suppression of the interference effects relative to the direct emissions.

To that aim, we shall estimate the contribution of the interference terms to the spectrum for medium-induced radiation for dipole angles $\theta_{q\bar{q}} \gg \theta_c$. This contribution is obtained by multiplying the Gaussian in Eq. (5.9) by the corresponding longitudinal phase-space $\tau_{min}\tau_f$, by the normalization $k^+/(x^+ - y^+) \sim \omega/\tau_f$ of the gluon propagator (5.6), and by a factor θ_f^2 which estimates the transverse derivatives in Eq. (5.2). As in Sect. 2.2, $\tau_{min} \equiv \min(\tau_{int}, \tau_{coh})$ is the smallest among the coherence scales which limit y^+ in the context of interference: $\tau_{min} = \tau_{int}$ when $\theta_{q\bar{q}} \gtrsim \theta_f$ and, respectively, $\tau_{min} = \tau_{coh}$ when $\theta_c \ll \theta_{q\bar{q}} \lesssim \theta_f$. The angular factor θ_f^2 is the same as for direct emissions. In the present context, this factor is not *a priori* obvious and will be later checked via explicit calculations. But before doing that, let us first exhibit the interference contribution to the spectrum, which reads (for $k_\perp \gtrsim k_f$)

$$\mathcal{I}^{(in)}(\omega, \mathbf{k}_\perp) \propto -\alpha_s C_F \theta_f^2 \tau_{min} \frac{\omega}{Q_s^2} \exp \left\{ -\frac{(\mathbf{k}_\perp - \Delta \mathbf{k}_\perp)^2}{Q_s^2} \right\}. \quad (5.14)$$

The off-set $\Delta \mathbf{k}_\perp$ in the Gaussian is obtained from the respective quantity in Eq. (5.6) after averaging over the emission times:

$$\Delta \mathbf{k}_\perp = k^+ \left\langle \frac{\mathbf{u}_\perp x^+ - \bar{\mathbf{u}}_\perp y^+}{x^+ - y^+} \right\rangle \simeq k^+ \mathbf{u}_\perp + k^+ (\mathbf{u}_\perp - \bar{\mathbf{u}}_\perp) \frac{\tau_{min}}{\tau_f}. \quad (5.15)$$

As rather obvious from the fact $\tau_{min}/\tau_f \ll 1$, the second term in the r.h.s. is negligible in all the interesting cases. Hence the ensuing off-set $\Delta \mathbf{k}_\perp \simeq k^+ \mathbf{u}_\perp$ is the same as for direct emissions by the *quark*, cf. Eq. (4.21), although we have considered here a contribution to interference where the gluon is truly emitted by the *antiquark*. This interplay is in agreement with our physical picture that, in order to allow for interferences, the gluon emitted by the antiquark must be co-moving with the quark. Clearly, for the reversed situation, where the gluon is emitted by the quark (and thus is co-moving with the antiquark), one would obtain $\Delta \mathbf{k}_\perp \simeq k^+ \bar{\mathbf{u}}_\perp$.

By taking the ratio between the interference term (5.14) and the spectrum (4.21) for a direct emission by the quark, one finds, for $k_f \lesssim k_\perp \lesssim Q_s$,

$$\mathcal{R}(\omega, \mathbf{k}_\perp) \equiv \frac{|\mathcal{I}^{(in)}|}{\mathcal{P}_q^{(in)}} \simeq \frac{\tau_{min}}{L}, \quad (5.16)$$

which in turn implies

$$\left(\frac{\omega}{\omega_c} \right)^{1/2} \gtrsim \mathcal{R}(\omega, k_\perp) \gtrsim \frac{\omega}{\omega_c} \quad \text{when} \quad \theta_f \lesssim \theta_{q\bar{q}} \lesssim \theta_s, \quad (5.17)$$

for relatively large dipole angles $\theta_{q\bar{q}} \gtrsim \theta_f$ where $\tau_{min} = \tau_{int}$, and respectively

$$1 \gg \mathcal{R}(\omega, k_\perp) \gtrsim \left(\frac{\omega}{\omega_c} \right)^{1/2} \quad \text{when} \quad \theta_c \ll \theta_{q\bar{q}} \lesssim \theta_f, \quad (5.18)$$

for smaller angles, $\theta_c \lesssim \theta_f$, where $\tau_{min} = \tau_{coh}$. Eqs. (5.16)–(5.18) explicitly show the suppression of the interference effects relative to the direct emissions for the medium-induced radiation of the dipole and confirm the respective estimates in Sect. 2.2.

To complete the argument, one still needs to evaluate the transverse derivatives appearing in Eq. (5.2), that is

$$(u^i + i\partial_x^i/k^+)(\bar{u}^i - i\partial_y^i/k^+) \mathcal{K}_{q\bar{q}}(x^+, \mathbf{b}_\perp + \mathbf{x}_\perp; y^+, \mathbf{y}_\perp; k^+) \quad (5.19)$$

with the derivatives evaluated at $\mathbf{x}_\perp = \mathbf{u}_\perp x^+$ and $\mathbf{y}_\perp = \bar{\mathbf{u}}_\perp y^+$. Like in the corresponding calculation for direct emission, Eq. (4.19), we can replace $\mathcal{K}_{q\bar{q}} \rightarrow \mathcal{G}_0$ to obtain a parametric estimate. This yields

$$(u^i + i\partial_x^i/k^+)(\bar{u}^i - i\partial_y^i/k^+) \mathcal{G}_0 \rightarrow \left(u^i - \frac{b^i + u^i x^+ - \bar{u}^i y^+}{x^+ - y^+} \right) \left(\bar{u}^i - \frac{b^i + u^i x^+ - \bar{u}^i y^+}{x^+ - y^+} \right) + \frac{2i}{k^+(x^+ - y^+)}. \quad (5.20)$$

The last term in the r.h.s. is of order $1/(k^+ \tau_f) \sim \theta_f^2$. For small dipole angles $\theta_{q\bar{q}} \ll \theta_f$ it is easy to check that this is the dominant term. So, in what follows we focus on the less trivial case where $\theta_{q\bar{q}} \gg \theta_f$. Then one can use $y^+ \simeq \tau_{int} \ll x^+ \simeq \tau_f$ and $b_\perp \sim 1/Q_s$ to simplify the algebra. The terms within the brackets in the r.h.s. of Eq. (5.20) thus yield

$$\frac{[b^i - (\bar{u}^i - u^i)y^+][b^i - (\bar{u}^i - u^i)x^+]}{(x^+ - y^+)^2} \simeq \frac{\mathbf{b}_\perp \cdot (\mathbf{u}_\perp - \bar{\mathbf{u}}_\perp) + \tau_{int}(\mathbf{u}_\perp - \bar{\mathbf{u}}_\perp)^2}{\tau_f}. \quad (5.21)$$

Using $(\mathbf{u}_\perp - \bar{\mathbf{u}}_\perp)^2 \sim \theta_{q\bar{q}}^2$ together with Eq. (2.18), it becomes clear that the last term above is of order θ_f^2 . As for the first term, this is estimated as (after performing the \mathbf{b}_\perp -integration, cf. Eq. (5.9))

$$\frac{(\mathbf{k}_\perp - k^+ \mathbf{u}_\perp) \cdot (\mathbf{u}_\perp - \bar{\mathbf{u}}_\perp)}{Q_s^2 \tau_f} \lesssim \frac{\omega \theta_q \theta_{q\bar{q}}}{Q_s^2 \tau_f} \sim \theta_f^2 \frac{\theta_q \theta_{q\bar{q}}}{\theta_s^2} \lesssim \theta_f^2. \quad (5.22)$$

We have also used here Eq. (4.18) together with the relations $k_f^2 \sim \omega/\tau_f$ and $k_f/Q_s = \theta_f/\theta_s$. To conclude, the dominant effect of the transverse derivatives in the interference terms is a factor θ_f^2 , so like for the direct emissions.

6. Discussion and outlook

Throughout this work, we have mostly focussed on medium-induced radiation of the BDMPS-Z type, whose main characteristic is that the gluons are emitted *inside* the medium, as a result of multiple scattering. However, we have also noticed at several places that this is not the only type of medium-induced radiation for the case of a dense medium. Indeed, as found in Refs. [26, 27] (and reviewed in our Sect. 3.2), the color decoherence of the $q\bar{q}$ antenna leads to additional radiation *outside* of the medium, which is localized in a region of (angular) phase space that would be forbidden — by destructive interference — in the vacuum. The essential reason why this new type of radiation exists is because the characteristic time scale τ_{coh} beyond which the $q\bar{q}$ pair loses its color coherence becomes much smaller than the vacuum-like formation time for a gluon radiated outside the dipole cone, which is typically $\tau_{int} = 2/(\omega\theta_{q\bar{q}}^2)$. However, according to Eq. (2.18), the inequality $\tau_{coh} \ll \tau_{int}$ holds whenever $\theta_{q\bar{q}} \ll \theta_f$, which allows for (vacuum) formation times τ_{int} that are both larger *and* smaller than the medium size L . Hence, the

same mechanism could in principle lead to additional gluon radiation *inside* the medium. This possibility has not been mentioned in the previous literature, so we shall succinctly explore it here, via qualitative considerations based on our previous results.

Specifically, one has $\tau_{int} \simeq L$ when $\theta_{q\bar{q}} \simeq \theta_{out}$, where

$$\theta_{out} \equiv \sqrt{\frac{2}{\omega L}} = \theta_c \sqrt{\frac{\omega_c}{\omega}} = \theta_f \left(\frac{\omega}{\omega_c} \right)^{1/4}, \quad (6.1)$$

is the same as the upper limit in our Eq. (3.31). So, *a priori* there are two angular regions where the mechanism proposed in Refs. [26, 27] could operate¹¹: (1) $\theta_c \ll \theta_{q\bar{q}} \lesssim \theta_{out}$, where $\tau_{int} \gtrsim L$, so the respective emissions take place *outside* the medium; this is the situation considered in [26, 27] and (2) $\theta_{out} \ll \theta_{q\bar{q}} \ll \theta_f$ where $\tau_{int} \ll L$, so the gluons are emitted (via vacuum-like processes) *inside* the medium; this is the new possibility that we would like to explore. Note that, together, these two angular domains completely overlap with our region of ‘relatively small dipole angles’ for BDMPS–Z radiation, as defined in Sect. 2.2. This observation naturally leads to the following two questions: (a) what is the dominant mechanism for medium-induced radiation for dipole angles within this common range at $\theta_c \ll \theta_{q\bar{q}} \ll \theta_f$, and (b) what are the most interesting values of $\theta_{q\bar{q}}$ for applications to the phenomenology? These are the main questions that we would like to address in this section.

With respect to the first question above, its answer depends upon the ration $\theta_{q\bar{q}}/\theta_{out}$, as we argue now. When $\theta_c \ll \theta_{q\bar{q}} \lesssim \theta_{out}$, that is, in region (1) above, the radiation due to the new mechanism of Refs. [26, 27] is concentrated *outside* the dipole cone, but relatively *close to it*: indeed, this radiation has the angular distribution of the usual bremsstrahlung spectrum, that is, it is strongly peaked around the sources and it decays as $1/\theta$ at large emission angles $\theta \gg \theta_{q\bar{q}}$. By contrast, the BDMPS–Z gluons are emitted at relatively large angles $\theta_f \gg \theta_{out}$ w.r.t. their sources, meaning far outside the dipole cone. Hence in range (1) for $\theta_{q\bar{q}}$, both types of medium-induced radiation exist, but they are widely separated in angle from each other: the out-of-medium emissions dominate the spectrum for $\theta_q, \theta_{\bar{q}} \sim \theta_{q\bar{q}}$, while the in-medium emissions à la BDMPS–Z dominate for $\theta_q, \theta_{\bar{q}} \sim \theta_f$.

Consider now larger dipole angles, $\theta_{out} \ll \theta_{q\bar{q}} \ll \theta_f$ (the angular region (2)). Then the previous discussion of the BDMPS–Z gluons goes unchanged, whereas the mechanism proposed in Refs. [26, 27] is expected to become ineffective: indeed, in-medium radiation with small emissions angles $\theta_{q\bar{q}} \ll \theta_f$ and hence relatively large formation time $\tau_{int} \gg \tau_f$ is strongly suppressed as compared to the BDMPS–Z radiation, since the soft gluons cannot avoid accumulating transverse momenta of order k_f , via medium rescattering; as a consequence, they are liberated from the parent quark after a relatively short time τ_f and at an angle $\sim \theta_f$. Hence, for dipole angles within region (2), the medium-induced radiation is predominantly of the BDMPS–Z type and is distributed at large angles $\theta \gtrsim \theta_f \gg \theta_{q\bar{q}}$, far outside the dipole cone.

These considerations show that the physical consequences of the two mechanisms for medium-induced radiation should be quite different: whereas the BDMPS–Z gluons are more effective in broadening the energy distribution of a jet in the transverse plane, in qualitative agreement with the observations at the LHC [2, 3], the mechanism proposed in [26, 27] is probably more important for the softening of the intra-jet radiation and its redistribution at small angles. But

¹¹We recall that the lower limit θ_c on $\theta_{q\bar{q}}$ comes from the condition that $\tau_{coh} \ll L$, cf. Eq. (2.17).

a more detailed phenomenological analysis is still needed before drawing firm conclusions on the last point.

Since the in-medium antenna pattern is so sensitive to the value of the dipole angle, it is important to estimate what are the relevant values in the context of heavy ion collisions. A physical process where in-medium, color-singlet, antennas like the one that we have discussed are naturally generated is the hadronic decay of a heavy vector boson like the Z or the W. In this scenario, the dipole angle of the pair depends upon the boson kinematics, in particular, on its boost: $\theta_{q\bar{q}} \sim 1/\gamma$. However, while such bosons are copiously produced in Pb+Pb collisions at the LHC, their identification via hadronic decays is complicated, if at all possible, by the large QCD background¹².

Another source of in-medium antennas, but typically in non-singlet color representations, is the evolution of jets produced via hard processes in heavy collisions. Although our calculations have been restricted to the color singlet case, our arguments are sufficiently general to be applicable to a qualitative discussion of antennas in other representations. We expect no modification in the physical regimes for interference and the associated angular ranges summarized in Sect. 2.2. In particular, for relatively large angles $\theta_{q\bar{q}} \gg \theta_c$ our main conclusion remains unchanged: the interference effects are suppressed and the overall antenna pattern is the sum of two independent BDMPS-Z spectra produced by the two legs of the antenna. For smaller angles, on the other hand, the interference effects *are* important and their result is such that, when $\theta_{q\bar{q}} \ll \theta_c$, the total in-medium radiation by the antenna coincides with that by a single source which carries the global color charge of the antenna (e.g., a source in the adjoint representation if the antenna was produced by a gluon decay). It would be interesting to check this conclusion explicitly. (The calculation of the octet channel in [27] provides a partial check in that sense.)

Within the in-medium jet evolution we can distinguish two types of antennas: those generated via hard, vacuum-like, parton splittings and those arising via medium-induced emissions. Addressing the relevant angles in either case will ultimately resort on in-medium Monte-Carlo generators, such as [33, 34, 35, 36, 37, 38], which can keep track of all the kinematical and probabilistic effects. Here we will provide some simple estimates based on physical arguments, to be ultimately confronted to explicit calculations. For simplicity, we shall treat \hat{q} as a fixed parameter in these estimates, in lines with our general strategy throughout this paper.

Consider first an antenna resulting from medium-induced radiation. The main question is, what is the typical angle between the emitted gluon and the parent parton *by the time of a subsequent gluon emission*. This angle starts with a value $\sim \theta_f$ at the time of formation but it can be enlarged by additional multiple scattering occurring after the formation. So, we need to estimate the typical time interval τ_{rad} between two successive emissions. The probability for emitting a new gluon can be estimated as $\mathcal{P} \sim \alpha_s C_R n_{\text{eff}}$ where $n_{\text{eff}} \equiv \tau_{rad}/\tau_f$ is the number of effective scattering centers along τ_{rad} . This probability becomes of $\mathcal{O}(1)$ when

$$\tau_{rad} \sim \frac{\tau_f}{\alpha_s C_R}. \quad (6.2)$$

This estimate is a bit simplistic, since emissions can happen at different frequencies and the relevant probability is the inclusive one. Since the number of emitted gluons grows with decreasing

¹²We thank P. Quiroga, S. Sapeta and G. Soyez for useful discussions on this topic.

ω , cf. Eq. (2.7), a more realistic estimate (or, at least, a strict lower limit) reads

$$\tau_{rad} > \frac{\tau_f(\omega_{min})}{\alpha_s C_R} \sim \frac{1}{\alpha_s C_R \omega_{min}}, \quad (6.3)$$

where $\omega_{min} \sim \hat{q}^{1/3}$ is the lowest energy for BDMPS–Z gluons. Thus, for gluon frequencies which are not parametrically larger (in α_s) than ω_{min} , the typical time between successive emissions is much larger than the formation time and the partons that form the antenna acquire significant momentum by the time of secondary emissions, increasing the angle of the effective dipole. Thus, medium–induced gluons lead, typically, to relatively large dipoles, following the classification of Sect. 2.2. Note also that for the medium–induced parton cascade, this radiation time τ_{rad} plays the role of an effective medium length. Hence that fact that $\tau_{rad} \gg \tau_f$ (at least for not too large frequencies) guarantees the validity of our central argument for the suppression of the interference terms (the suppression factor being τ_f/τ_{rad} in this case).

A different source of antennas propagating in the medium is the vacuum–like evolution of hard partons. This refers to the emission of gluons with large transverse momenta $k_\perp \gg Q_s$ (which cannot be produced via in–medium interactions) and hence very short formation times $\tau_q \ll \tau_f$ (for a given frequency). The precise values of the dipole opening depends on the kinematics of the intervening hard processes, in particular on their energy and virtuality. Indeed, for a hard parton of energy E and virtuality Q which emits a hard gluon carrying a fraction z of its energy, the angle of emission is

$$\theta_{hard}^2 \approx \frac{1}{z(1-z)} \frac{Q^2}{E^2}, \quad (6.4)$$

and the emission time is estimated via the uncertainty principle as

$$\tau_{hard} \sim \frac{E}{Q^2} \sim \frac{1}{z(1-z)} \frac{1}{\theta_{hard}^2 E}. \quad (6.5)$$

(Using $\omega \simeq zE$ for a small– z emission and $\omega\theta_{hard} \simeq k_\perp$, it becomes clear that Eq. (6.5) is consistent with our basic formula (2.1) for the formation time.) Thus, unless the branchings are very asymmetric, the vacuum–like evolution can produce antennas with very small angles and at very early times $\tau_{hard} \ll L$. We conclude that light jets (those with jet mass much smaller than their total energy) can be sources for all the different types of dipoles discussed in Sect. 2.2, with a predilection though for small and very small dipoles in the sense of that discussion. Depending upon the precise relation between the emission angle θ_{hard} and the characteristic medium angle θ_c , the antenna created via such a hard branching can either act as a set of two independent sources of BDMPS–Z gluons (if $\theta_{hard} \gg \theta_c$), or radiate such gluons in the same way as the parent parton would do (if $\theta_{hard} \lesssim \theta_c$).

So far, we have discussed the in–medium hard branchings only as a mechanism for generating antennas, but we have not addressed the medium effects on such a branching by itself. As a matter of facts, we do not expect such effects to be significant: the in–medium emissions of relatively hard gluons with transverse momenta $k_\perp \gg Q_s$ should proceed exactly as in the vacuum, for both direct emissions and the corresponding interference phenomena leading to angular ordering. This is quite clear from the fact that the respective formation time τ_{hard} is much shorter than the time scale τ_{coh} for the color decoherence of the sources. Since there was

some confusion on this point in the recent literature [39], we would like to take this opportunity and fully clarify this issue. The analysis in Ref. [39] was based on the assumption that the color decorrelation time (the analog of our τ_{coh}) is to be identified with the mean free path ℓ of a colored parton propagating through the medium (as introduced in the discussion in Sect. 2.1). That assumption would be correct if and only if the two emitters which form the antenna would undergo *independent* color rotations in the medium, which in turn requires their transverse separation $r_\perp \sim \tau_q \theta_{q\bar{q}}$ at the time of emission to be larger the Debye screening length μ_D^{-1} . Clearly, this would be the case only for extremely soft radiated gluons, with transverse momenta $k_\perp \simeq \omega \theta_{q\bar{q}} \lesssim \mu_D$. For the medium created in heavy ion collisions at the current energies, this scale μ_D is of the order of a few hundred MeV. Gluons with such momenta are truly soft and do not significantly contribute to the in-medium evolution of a hard jet, which rather proceeds via hard, vacuum-like, emissions and semi-hard, medium-induced, ones.

Acknowledgments

We would like to thank Al Mueller for insightful and patient explanations on the BDMPS-Z physics, and Andrei Leonidov, Cyrille Marquet, Guilherme Milhano, Carlos Salgado, and Urs Wiedemann for many related discussions and useful comments on the manuscript.

A. Momentum space analysis of the gluon spectrum

The total radiation probability from the dipole, which includes the direct emissions from the quark, Eq. (4.7), and the antiquark (as obtained by replacing $u \rightarrow \bar{u}$ within Eq. (4.7)) and the quark-antiquark interference terms, Eq. (5.2), can be compactly expressed as

$$\mathcal{P}_{tot}^{(in)} = 2g^2 C_F \text{Re} \sum_{F, L=q, \bar{q}} \text{Sign}(F, L) \times \quad (\text{A.1})$$

$$\int_0^{L^+} dx^+ \int_0^{x^+} dy^+ \int d^2 \mathbf{b}_\perp e^{i \mathbf{k}_\perp \cdot \mathbf{b}_\perp} S_{gg}(L^+, x^+; \mathbf{b}_\perp) S_{F,L}(y^+, \mathbf{0}) I_{u_L, u_F}(x^+, y^+, \mathbf{b}_\perp)$$

(Note a slight change in the notations for the quark 4-velocities as compared to the main text: we identify $u_q \equiv u$ and $u_{\bar{q}} \equiv \bar{u}$. To avoid cumbersome notations, we shall indicate the transverse components of u_F and u_L by boldface symbols without the ‘ \perp ’ subscript: \mathbf{u}_F and \mathbf{u}_L .) The quark-quark dipole is trivial when both indexes are the same ($S_{qq} = S_{\bar{q}\bar{q}} = 1$) and the function $\text{Sign}(F, L) = 1$ if $F = L$ and $\text{Sign}(F, L) = -1$ otherwise¹³. These four terms summarize the four possible combinations appearing in the total emission probability which are the direct emissions from either the quark or the antiquark (Fig 5) and the two interference terms in which the gluon is first emitted, at time y^+ , by the fermion (quark or antiquark) which has velocity u_F and then absorbed, at time x^+ , by the other fermion (antiquark or quark), with velocity u_L (Fig. 7). The function $I_{u_L, u_F}(x^+, y^+, \mathbf{b}_\perp)$ encodes the quark-gluon dipole together with its transverse derivatives:

$$I_{u_L, u_F}(x^+, y^+, \mathbf{b}_\perp) = e^{i \mathbf{k}^+ (u_L^- x^+ - u_F^- y^+)} (u_L^i + i \partial_x^i / k^+) (u_F^i - i \partial_y^i / k^+) \quad (\text{A.2})$$

$$\mathcal{K}_{qg}(x^+, \mathbf{x}_\perp + \mathbf{b}_\perp; y^+, \mathbf{y}_\perp; k^+) \Big|_{\mathbf{x}_\perp = \mathbf{u}_L x^+, \mathbf{y}_\perp = \mathbf{u}_F y^+}$$

¹³Eq. (4.7) corresponds to the term $u_L = u_F = u$ and Eq. (5.2) is obtained by setting $u_L = u$ and $u_F = \bar{u}$. A change of variables $\mathbf{b}_\perp = \mathbf{z}_\perp - \mathbf{x}_\perp$ has been also performed.

For the case of direct emissions, where u_L and u_F coincide with each other, the qg dipole is made with the gluon and the quark which has emitted that gluon (the *parent* quark). For the interference terms, this dipole is made with the gluon emitted by the quark with velocity u_F and the *other* quark, which has a velocity u_L .

We restrict ourselves to the case the ‘harmonic approximation’, in which the slowly varying logarithm ρ which enters the various dipole S -matrices (see e.g. Eqs. (4.4) and (4.6)) is treated as a fixed quantity, which is moreover absorbed into the normalization of \hat{q} . In this approximation, the quark–gluon path integral (Eq. (4.3)) is exactly known [11, 19] for the case of a single emitter with vanishing transverse velocity. The generalization to the present case, where the quark which enters the quark–gluon dipole possesses a non-zero transverse velocity \mathbf{u}_L , is easily to find and reads

$$\begin{aligned} \mathcal{K}_{qg}(x^+, \mathbf{x}_\perp; y^+, \mathbf{y}_\perp; k^+) &= e^{-ik^+u_L^-(x^+-y^+)+ik^+\mathbf{u}_L\cdot(\mathbf{x}-\mathbf{y})_\perp} \\ &\times \frac{A}{2\pi} \exp \left\{ -\frac{A}{2} (B(\bar{\mathbf{x}}_\perp^2 + \bar{\mathbf{y}}_\perp^2) - 2\bar{\mathbf{x}}_\perp \cdot \bar{\mathbf{y}}_\perp) \right\} \Big|_{\bar{\mathbf{x}}_\perp = \mathbf{x}_\perp - \mathbf{u}_L x^+, \bar{\mathbf{y}}_\perp = \mathbf{y}_\perp - \mathbf{u}_L y^+} \end{aligned} \quad (\text{A.3})$$

where Ω has been already defined in Eq. (4.8) and we have introduced

$$A \equiv \frac{k^+\Omega}{i \sinh \Omega (x^+ - y^+)}, \quad B \equiv \cosh \Omega (x^+ - y^+). \quad (\text{A.4})$$

A.1 The gluon spectrum at the time of formation

The quark–gluon dipole encodes the process of in-medium gluon formation. Right after formation, the gluon spectrum is obtained via the Fourier transform of Eq. (A.2). After some lengthy but straightforward algebra, we obtain

$$\begin{aligned} I_{u_L, u_F}(x^+, y^+, \mathbf{q}_\perp) &= \frac{1}{B} \left[(\mathbf{v}_\perp - \mathbf{u}_L)^2 \frac{1}{B} + (\mathbf{v}_\perp - \mathbf{u}_L) \cdot (\mathbf{u}_L - \mathbf{u}_F) (1 + C\Omega y^+) \right] \\ &\times \exp \left\{ -iC \frac{k^+ (\mathbf{v}_\perp - \mathbf{u}_L)^2}{2\Omega} + i \frac{k^+}{2} (\mathbf{u}_L - \mathbf{u}_F)^2 (1 + C\Omega y^+) y^+ \right. \\ &\quad \left. + i \frac{k^+}{B} (\mathbf{v}_\perp - \mathbf{u}_L) \cdot (\mathbf{u}_L - \mathbf{u}_F) y^+ \right\}, \end{aligned} \quad (\text{A.5})$$

where $\mathbf{v}_\perp \equiv \mathbf{q}_\perp/k^+$ is the gluon transverse velocity when it is formed and $C \equiv \tanh \Omega (x^+ - y^+)$ has the properties that $C/\Omega \simeq x^+ - y^+$ when $x^+ - y^+ \ll \tau_f$ and $C \rightarrow 1$ when $x^+ - y^+ \gg \tau_f$. (Recall that $\tau_f \equiv 1/|\Omega|$, cf. Eq. (4.11).)

The analysis of this expression shows the main features of the gluon spectrum *at the time of formation*. For $x^+ - y^+ \simeq \tau_f$, which is the typical value fixed by the subsequent integrations over x^+ and y^+ , one can write $C\Omega \approx 1/\tau_f$ to parametric accuracy, and then the first term in the exponent is parametrically the same as

$$\exp \left\{ -i \frac{k^+ (\mathbf{v}_\perp - \mathbf{u}_L)^2}{2\tau_f} \right\} = \exp \left\{ -i \frac{(\mathbf{q}_\perp - k^+ \mathbf{u}_L)^2}{2k_f^2} \right\}. \quad (\text{A.6})$$

Hence, for both the interference and the direct terms, the *transverse momentum distribution* is a Gaussian with width $k_f^2 \sim \sqrt{\omega \hat{q}}$ centered around the direction \mathbf{u}_L of the quark which enters the

quark–gluon dipole. (Note that, in the interference term, this is *not* the quark which emitted the gluon, but the other quark.)

Concerning the *angular structure* of the spectrum, as encoded in the first line of Eq. (A.5), this is a natural generalization of the corresponding result in the vacuum, to which it reduces, as it should, in the limit $|\Omega| \rightarrow 0$. Indeed, in that limit, $B \rightarrow 1$, $C \rightarrow 0$, so the expression within the square brackets becomes $(\mathbf{v}_\perp - \mathbf{u}_L) \cdot (\mathbf{v}_\perp - \mathbf{u}_F)$; this is the expected result for both the direct terms, cf. Eq. (3.21), and the interference ones, cf. Eq. (3.23). (Of course, in the vacuum, the gluon velocity at the time of formation is the same as its *final* velocity.) One can similarly check that, when $|\Omega| \rightarrow 0$, the exponent in Eq. (A.5) reduces to the respective vacuum result, *i.e.*, to the formation–time phases visible e.g. in Eq. (5.8).

In addition to the angle and momentum distributions, Eq. (A.5) also shows what are the *time scales* involved in the radiation process. The overall prefactor $1/B$, which at long times behaves as $1/B \sim \exp\{-\Omega(x^+ - y^+)\}$, sets the *formation* time of the gluons as $x^+ - y^+ \simeq \tau_f$, in agreement with Eq. (2.4). The other relevant time scale is the typical value of the *first emission* time y^+ (more properly, this is the time at which the gluon formation is initiated). For direct emissions ($\mathbf{u}_L = \mathbf{u}_F$), there is no characteristic value of y^+ and emissions happen all along the medium length with equal probability. By contrast, for the interference terms ($\mathbf{u}_L \neq \mathbf{u}_F$), the values of y^+ are constrained by two new time scales, τ_λ and τ_{int} , which are generated by the middle term in the exponent in Eq. (A.5) and its interplay with the other terms.

Specifically, for $x^+ - y^+ \simeq \tau_f$, one can write $1 + C \Omega y^+ \approx (\tau_f + y^+)/\tau_f \approx x^+/\tau_f$ to parametric accuracy, and hence

$$\frac{ik^+}{2} (\mathbf{u}_L - \mathbf{u}_F)^2 (1 + C \Omega y^+) y^+ \approx i \frac{k^+ \theta_{q\bar{q}}^2 x^+ y^+}{4\tau_f}. \quad (\text{A.7})$$

This is clearly equivalent with the first factor in Eq. (5.11). As explained in Sects. 2.2 and 5, this term encodes *two* time scales: τ_λ , which is an upper limit on $\sqrt{y^+(y^+ + \tau_f)}$ for generic values of $\theta_{q\bar{q}}$, cf. Eq. (5.12), and τ_{int} , which is the ensuing limit on y^+ for relatively large angles $\theta_{q\bar{q}} \gg \theta_f$, cf. Eq. (5.13). The last term in the exponent in Eq. (A.5), which involves the momentum acquired by the gluon during formation, leads to the same time scale τ_λ , as clear from the fact that $k^+ |\mathbf{v}_\perp - \mathbf{u}_L| \sim \omega \theta_f$ for the typical gluon velocity \mathbf{v}_\perp . Finally, in addition to Eq. (A.5), the time dependence of the interference term is also sensitive to the overall suppression due to the initial $q\bar{q}$ dipole, Eq. (5.3), which introduces the additional time scale τ_{coh} for color decoherence.

At this level, it is straightforward to make contact between Eq. (A.5) and the expression (2.7) for the ‘formation’ spectrum deduced in Sect. 2.2 via qualitative arguments: for direct emissions, the only surviving term in the first line of Eq. (A.5) is $(\mathbf{v}_\perp - \mathbf{u}_L)^2 \simeq \theta_q^2$. To compute the spectrum at the formation time, one needs to perform the time integrations in Eq. (A.1) *without* the factor S_{gg} there, which describes multiple scattering *after* formation. For $\tau_f \ll L$ the integral over the time difference $x^+ - y^+$ is cut off by the factor $1/B^2$ and yields a factor τ_f , while the subsequent integral over y^+ is unrestricted and yields a factor L . Altogether, we have a factor $\theta_f^2 \tau_f L$ multiplying the Gaussian in Eq. (A.6) plus, of course, the overall factor $\alpha_s C_F$. This reproduces the parametric estimate in Eq. (2.7).

A.2 The final gluon spectrum

The previous arguments also show that, in order to compute the *final* spectrum, as it would

be measured by a detector, one needs to also take into account the S -matrix S_{gg} of gg dipole. Working in the momentum representation, the final spectrum is obtained by convoluting the spectrum at the time of formation with the Fourier transform of S_{gg} . Within the ‘harmonic approximation’, this amounts to an additional Gaussian broadening:

$$F_{u_L, u_F}(x^+, y^+, \mathbf{k}_\perp) = \int \frac{d^2 \mathbf{q}_\perp}{(2\pi)^2} I_{u_L, u_F}(x^+, y^+, \mathbf{q}_\perp) \frac{4\pi}{Q_s^2} e^{-(\mathbf{k}_\perp - \mathbf{q}_\perp)^2 / Q_s^2} \quad (\text{A.8})$$

where $Q_s^2 \equiv \hat{q}(L^+ - x^+)$ depends upon the final formation time x^+ . Since the typical gluons are produced within the bulk of the medium ($x^+ \ll L^+$), one can neglect the x^+ -dependence of Q_s^2 to parametric accuracy. After also using $\tau_f \ll L$, we find (with $Q_s^2 = \hat{q}L^+$ from now on)

$$\begin{aligned} F_{u_L, u_F}(x^+, y^+, \mathbf{k}_\perp) &\approx \quad (\text{A.9}) \\ &\approx \frac{2k^+ \Omega}{B Q_s^2} \left[\frac{2}{B} \frac{\Omega}{ik^+} + \frac{y^+ \Omega (\mathbf{u}_L - \mathbf{u}_F)^2}{\sinh \Omega(x^+ - y^+)} \left(1 + y^+ \Omega \left(1 + \frac{2}{B} \right) \right) - \right. \\ &\quad \left. - 2i \frac{\Omega}{Q_s^2} (\mathbf{k}_\perp - k^+ \mathbf{u}_L) \cdot (\mathbf{u}_L - \mathbf{u}_F) \left(1 + y^+ \Omega \left(1 + \frac{4}{B} \right) \right) \right] \times \\ &\quad \exp \left\{ i \frac{k^+}{2} (\mathbf{u}_L - \mathbf{u}_F)^2 (1 + \Omega y^+) y^+ - \frac{1}{Q_s^2} \left(\mathbf{k}_\perp - k^+ \mathbf{u}_L - \frac{k^+ \Omega y^+ (\mathbf{u}_L - \mathbf{u}_F)}{\sinh \Omega(x^+ - y^+)} \right)^2 \right\}, \end{aligned}$$

where we have further approximated $C \approx 1$ since we anticipate that $x^+ - y^+ \simeq \tau_f$. To understand Eq. (A.9) to parametric accuracy, one can also set $B \approx 1$ and $\sinh \Omega(x^+ - y^+) / \Omega \approx \tau_f$.

As before, the first line of Eq. (A.9) specifies the angular dependence of the final spectrum. Unlike in Eq. (A.5), there is not a term proportional to the square of the final angle formed by the gluon and the quark. This is so since the final gluon spectrum receives contributions from the entire gluon spectrum at formation. The final distribution is characterized by θ_f , the typical angle at formation, which can be identified in the first term of this line: $|\Omega|/k^+ = 1/(\tau_f k^+) \simeq \theta_f^2$. For the interference term there is, however, a residual dependence upon the final direction of the gluon: this enters via the middle line of Eq. (A.9), which is due to the fact that there is some correlation between the final direction of the gluon and its direction at the time of emission (as encoded in the off-set $k^+ \mathbf{u}_L$ in the final gluon momentum). This term is essentially the same as that in Eq. (5.22) from the main text and, as shown there, it is generally subleading.

The last line in Eq. (A.9) encode both the time and momentum dependence. The first term in the exponent was already present in Eq. (A.5) (the middle term in the exponent there) and, as already explained, it encodes the condition of quantum coherence — that is, the two time scales τ_λ and τ_{int} . The second term in the exponent shows the transverse momentum spectrum, which is a Gaussian of width Q_s^2 around the direction \mathbf{u}_L of the quark which participates in the formation process (*i.e.*, the quark from the qg dipole). The \mathbf{q}_\perp -dependence of the exponent in Eq. (A.9) leads to a shift in the center of the transverse momentum gaussian; in fact, by using $\sinh \Omega(x^+ - y^+) / \Omega \approx \tau_f$ to parametric accuracy, one sees that this additional shift is the same as the second term in the r.h.s. of Eq. (5.15). As will be later verified, this additional shift is negligible in all the interesting cases.

Note finally that, as in the case of the spectrum at formation, Eq. (A.9) must be supplemented with the qg dipole Eq. (5.3), which introduces the coherence time. We will now

specify the parametric dependence of the radiation spectrum for the different terms in the gluon amplitude.

A.3 Direct emission: the BDMPS–Z spectrum

In the case of direct emission by either the quark or the antiquark, the final spectrum is obtained by integrating the following expression

$$F_q(x^+, y^+, \mathbf{k}_\perp) \simeq \frac{4\Omega^2}{iQ_s^2} \frac{1}{B^2} \exp \left\{ -\frac{(\mathbf{k}_\perp - k^+ \mathbf{u}_\perp)^2}{Q_s^2} \right\} \quad (\text{A.10})$$

over the time variables x^+ and y^+ . For definiteness, we have shown here the direct emission by the quark but there is of course a similar contribution by the antiquark. As expected, at this level of approximation the spectrum is a Gaussian centered around the transverse momentum $k^+ \mathbf{u}_\perp$ inherited from the parent parton. As already explained, the subsequent integrations over the time variables introduce a factor $\tau_f L$. By also using $\tau_f \sim 1/|\Omega|$ and $\theta_f^2 \sim |\Omega|/k^+$ we recover the parametric dependencies shown in Eq. (4.21) of the main text.

A.4 The interference terms for relatively large dipoles: $\theta_f \lesssim \theta_{q\bar{q}} \lesssim \theta_s$.

We shall now provide estimates for the interference contributions to the gluon spectrum, as obtained by integrating the expression in Eq. (A.9) with $\mathbf{u}_L \neq \mathbf{u}_F$ over the time variables x^+ and y^+ . We first consider dipole angles within the range $\theta_f \lesssim \theta_{q\bar{q}} \lesssim \theta_s$. As before, the integration over $x^+ - y^+$ is dominated by τ_f . But unlike the previous case of direct emissions, the y^+ -integration is now more complicated since there are several competing time scales. As we have extensively discussed in Sect. 2.2, within the present range for dipole angles, the relevant time scales are strictly ordered, $\tau_{int} \lesssim \tau_\lambda \lesssim \tau_{coh} \lesssim \tau_f$, and the integral over y^+ is controlled by the smallest time scale, τ_{int} . In addition, since $\tau_{int}/\tau_f \ll 1$, all terms proportional to $y^+ \Omega$ in Eq. (A.9) can be neglected. Then the only dependence upon y^+ which survives in the exponent is that encoded in the first term there, $\simeq ik^+ \theta_{q\bar{q}}^2 y^+$, which after integration yields a factor τ_{int} , as expected. The same approximations allow us to simplify the angular dependence of the final spectrum (the first line of Eq. (A.9)) which contains terms proportional to θ_f^2 , $\theta_{q\bar{q}}^2$ and $\theta_L \theta_{q\bar{q}}$, where $\theta_L = \theta_q$ or $\theta_{\bar{q}}$ is the gluon angle with respect to the quark which enters the $q\bar{q}$ dipole. By also using $|\Omega|/k^+ \sim \theta_f^2$, $|\Omega|k^+ \sim k_f^2$ and the following estimates,

$$\begin{aligned} \tau_{int} |\Omega| \theta_{q\bar{q}}^2 &\sim \theta_f^2, \\ \frac{k_f^2}{Q_s^2} \theta_L \theta_{q\bar{q}} &\sim \theta_f^2 \frac{\theta_{q\bar{q}}^2 \theta_L}{\theta_s^2 \theta_{q\bar{q}}}, \end{aligned} \quad (\text{A.11})$$

one eventually finds that the total interference term is parametrically given by

$$\mathcal{I}^{(\text{in})}(\omega, k_\perp) \propto -\alpha_s C_F \theta_f^2 \left(1 - c_1 \frac{\theta_{q\bar{q}}^2 \theta_L}{\theta_s^2 \theta_{q\bar{q}}} \right) \tau_{int} \frac{\omega}{Q_s^2} \exp \left\{ -\frac{(k_\perp - k^+ \mathbf{u}_L)^2}{Q_s^2} \right\} \quad (\text{A.12})$$

where c_1 is a number of order one. We see that, unless θ_L is arbitrary large, $\theta_L \gg \theta_{q\bar{q}}$, the interference term, Eq. (A.12), is suppressed with respect to the direct term, Eq. (4.21), by

$$\frac{\tau_{int}}{L^+} \ll \frac{\tau_f}{L^+} \ll 1. \quad (\text{A.13})$$

Note that the term proportional to c_1 within the parentheses in Eq. (A.12) is the same as that appearing in Eq. (5.22) of the main text.

A.5 The interference terms for relatively small dipoles: $\theta_c \ll \theta_{q\bar{q}} \ll \theta_f$.

Consider similarly the other relevant range for the dipole angles, at $\theta_c \ll \theta_{q\bar{q}} \ll \theta_f$. Then, as discussed in Sect. 2.2, the ordering of time scales gets now reverted, $\tau_f \ll \tau_{coh} \ll \tau_\lambda \ll \tau_{int}$ and the y^+ integration is restricted by the smallest of the coherence time scales, that is τ_{coh} . In this case, one we can safely neglect the y^+ dependence of the exponential in Eq. (A.9). (The integral over y^+ is rather controlled by the $q\bar{q}$ dipole and yields a factor τ_{coh} .) In addition, since

$$\frac{(k^+)^2 \theta_{q\bar{q}}^2}{k_f^2} \frac{\tau_{coh}^2}{\tau_f^2} \sim \left(\frac{\theta_{q\bar{q}}}{\theta_f} \right)^{2/3} \ll 1, \quad (\text{A.14})$$

we can neglect the shift in the transverse momentum Gaussian in Eq. (A.9) for any final momentum $k_\perp \gtrsim k_f$. The overall magnitude of the interference term is controlled by the prefactor encoding the angular dependence (the first line in Eq. (A.9)). In the present case $\tau_{coh}|\Omega| \gg 1$ and we need to determine the relative value of the three different contributions to the spectrum. Simple manipulations show that

$$\begin{aligned} (\tau_{coh} \theta_{q\bar{q}} |\Omega|)^2 &\sim \theta_f^2 \left(\frac{\theta_{q\bar{q}}}{\theta_f} \right)^{2/3} \ll \theta_f^2 \\ \frac{k_f^2}{Q_s^2} \frac{\tau_{coh}}{\tau_f} \theta_L \theta_{q\bar{q}} &\sim \theta_f^2 \frac{\theta_L \theta_f}{\theta_s^2} \left(\frac{\theta_{q\bar{q}}}{\theta_f} \right)^{1/3}. \end{aligned} \quad (\text{A.15})$$

Using this expression and taking into account that the x^+ and y^+ integration lead to an overall factor of $\tau_f \tau_{coh}$ we can estimate the parametric dependence of the interference spectrum as

$$\mathcal{I}^{(\text{in})}(\omega, k_\perp) \propto -\alpha_s C_F \theta_f^2 \left(1 - c_2 \frac{\theta_L \theta_f}{\theta_s^2} \left(\frac{\theta_{q\bar{q}}}{\theta_f} \right)^{1/3} \right) \tau_{coh} \frac{\omega}{Q_s^2} \exp \left\{ -\frac{(k_\perp - k^+ \mathbf{u}_L)^2}{Q_s^2} \right\} \quad (\text{A.16})$$

where c_2 is a number of order 1. It is then clear that, unless one considers gluons emitted at very large angles $\theta_L \gg \theta_s$, the interference term is proportional to θ_f^2 and its magnitude is suppressed as compared to the direct term by

$$\frac{\tau_{coh}}{L} \sim \left(\frac{\theta_c}{\theta_{q\bar{q}}} \right)^{2/3} \ll 1. \quad (\text{A.17})$$

References

- [1] **Atlas Collaboration**, G. Aad *et al.*, ‘‘Observation of a Centrality-Dependent Dijet Asymmetry in Lead-Lead Collisions at $\sqrt{s(\text{NN})} = 2.76$ TeV with the ATLAS Detector at the LHC,’’ *Phys. Rev. Lett.* **105** (2010) 252303, [arXiv:1011.6182 \[hep-ex\]](#).
- [2] **CMS Collaboration**, S. Chatrchyan *et al.*, ‘‘Observation and studies of jet quenching in PbPb collisions at nucleon-nucleon center-of-mass energy = 2.76 TeV,’’ [arXiv:1102.1957 \[nucl-ex\]](#).
- [3] **STAR Collaboration** Collaboration, M. Ploskon, ‘‘Inclusive cross section and correlations of fully reconstructed jets in $s(\text{NN})^{1/2} = 200$ -GEV Au+Au and p+p collisions,’’ *Nucl.Phys.* **A830** (2009) 255C–258C, [arXiv:0908.1799 \[nucl-ex\]](#).
- [4] **BRAHMS Collaboration** Collaboration, I. Arsene *et al.*, ‘‘Quark gluon plasma and color glass condensate at RHIC? The Perspective from the BRAHMS experiment,’’ *Nucl.Phys.* **A757** (2005) 1–27, [arXiv:nucl-ex/0410020 \[nucl-ex\]](#).

- [5] B. B. Back *et al.*, “The PHOBOS perspective on discoveries at RHIC,” *Nucl. Phys.* **A757** (2005) 28–101, [arXiv:nuc1-ex/0410022](#).
- [6] **STAR Collaboration** Collaboration, J. Adams *et al.*, “Experimental and theoretical challenges in the search for the quark gluon plasma: The STAR Collaboration’s critical assessment of the evidence from RHIC collisions,” *Nucl.Phys.* **A757** (2005) 102–183, [arXiv:nuc1-ex/0501009](#) [nuc1-ex].
- [7] **PHENIX** Collaboration, K. Adcox *et al.*, “Formation of dense partonic matter in relativistic nucleus nucleus collisions at RHIC: Experimental evaluation by the PHENIX collaboration,” *Nucl. Phys.* **A757** (2005) 184–283, [arXiv:nuc1-ex/0410003](#).
- [8] **ALICE** Collaboration, K. Aamodt *et al.*, “Suppression of Charged Particle Production at Large Transverse Momentum in Central Pb–Pb Collisions at $\sqrt{s_{NN}} = 2.76$ TeV,” *Phys. Lett.* **B696** (2011) 30–39, [arXiv:1012.1004](#) [nuc1-ex].
- [9] R. Baier, Y. L. Dokshitzer, A. H. Mueller, S. Peigne, and D. Schiff, “Radiative energy loss of high energy quarks and gluons in a finite-volume quark-gluon plasma,” *Nucl. Phys.* **B483** (1997) 291–320, [arXiv:hep-ph/9607355](#).
- [10] R. Baier, Y. L. Dokshitzer, A. H. Mueller, S. Peigne, and D. Schiff, “Radiative energy loss and p(T)-broadening of high energy partons in nuclei,” *Nucl. Phys.* **B484** (1997) 265–282, [arXiv:hep-ph/9608322](#).
- [11] R. Baier, Y. L. Dokshitzer, A. H. Mueller, and D. Schiff, “Radiative energy loss of high energy partons traversing an expanding QCD plasma,” *Phys. Rev.* **C58** (1998) 1706–1713, [arXiv:hep-ph/9803473](#).
- [12] B. Zakharov, “Fully quantum treatment of the Landau-Pomeranchuk-Migdal effect in QED and QCD,” *JETP Lett.* **63** (1996) 952–957, [arXiv:hep-ph/9607440](#) [hep-ph].
- [13] M. Gyulassy, P. Levai, and I. Vitev, “Reaction operator approach to nonAbelian energy loss,” *Nucl.Phys.* **B594** (2001) 371–419, [arXiv:nuc1-th/0006010](#) [nuc1-th].
- [14] U. A. Wiedemann, “Gluon radiation off hard quarks in a nuclear environment: Opacity expansion,” *Nucl.Phys.* **B588** (2000) 303–344, [arXiv:hep-ph/0005129](#) [hep-ph].
- [15] C. A. Salgado and U. A. Wiedemann, “Medium modification of jet shapes and jet multiplicities,” *Phys. Rev. Lett.* **93** (2004) 042301, [arXiv:hep-ph/0310079](#).
- [16] E. Wang and X.-N. Wang, “Jet tomography of dense and nuclear matter,” *Phys.Rev.Lett.* **89** (2002) 162301, [arXiv:hep-ph/0202105](#) [hep-ph].
- [17] P. B. Arnold, G. D. Moore, and L. G. Yaffe, “Photon and gluon emission in relativistic plasmas,” *JHEP* **0206** (2002) 030, [arXiv:hep-ph/0204343](#) [hep-ph].
- [18] R. Baier, D. Schiff, and B. Zakharov, “Energy loss in perturbative QCD,” *Ann.Rev.Nucl.Part.Sci.* **50** (2000) 37–69, [arXiv:hep-ph/0002198](#) [hep-ph].
- [19] J. Casalderrey-Solana and C. A. Salgado, “Introductory lectures on jet quenching in heavy ion collisions,” *Acta Phys. Polon.* **B38** (2007) 3731–3794, [arXiv:0712.3443](#) [hep-ph].
- [20] D. d’Enterria, “Jet quenching,” [arXiv:0902.2011](#) [nuc1-ex].
- [21] A. Majumder and M. Van Leeuwen, “The theory and phenomenology of perturbative QCD based jet quenching,” [arXiv:1002.2206](#) [hep-ph].
- [22] J. Casalderrey-Solana, J. G. Milhano, and U. A. Wiedemann, “Jet Quenching via Jet Collimation,” *J.Phys.G* **G38** (2011) 035006, [arXiv:1012.0745](#) [hep-ph].

- [23] G.-Y. Qin and B. Muller, “Explanation of Di-jet asymmetry in Pb+Pb collisions at the Large Hadron Collider,” *Phys.Rev.Lett.* **106** (2011) 162302, [arXiv:1012.5280 \[hep-ph\]](#).
- [24] I. Lokhtin, A. Belyaev, and A. Snigirev, “Jet quenching pattern at LHC in PYQUEN model,” *Eur.Phys.J.C* (2011) , [arXiv:1103.1853 \[hep-ph\]](#).
- [25] C. Young, B. Schenke, S. Jeon, and C. Gale, “Dijet asymmetry at the Large Hadron Collider,” [arXiv:1103.5769 \[nucl-th\]](#).
- [26] Y. Mehtar-Tani, C. A. Salgado, and K. Tywoniuk, “Antiangular Ordering of Gluon Radiation in QCD Media,” *Phys. Rev. Lett.* **106** (2011) 122002, [arXiv:1009.2965 \[hep-ph\]](#).
- [27] Y. Mehtar-Tani, C. A. Salgado, and K. Tywoniuk, “Jets in QCD media: from color coherence to decoherence,” [arXiv:1102.4317 \[hep-ph\]](#).
- [28] Y. L. Dokshitzer, V. A. Khoze, A. H. Mueller, and S. I. Troian, “Basics of perturbative QCD,” Gif-sur-Yvette, France. Ed. Frontieres (1991) 274 p.
- [29] R. K. Ellis, W. J. Stirling, and B. R. Webber, “QCD and collider physics,” *Camb. Monogr. Part. Phys. Nucl. Phys. Cosmol.* **8** (1996) 435 p.
- [30] Y. Mehtar-Tani and K. Tywoniuk, “Jet coherence in QCD media: the antenna radiation spectrum,” [arXiv:1105.1346 \[hep-ph\]](#).
- [31] E. Iancu and R. Venugopalan, “The Color glass condensate and high-energy scattering in QCD,” [arXiv:hep-ph/0303204 \[hep-ph\]](#). In QGP3, Eds. R.C. Hwa and X.N.Wang, World Scientific.
- [32] Y. Mehtar-Tani, “Relating the description of gluon production in pA collisions and parton energy loss in AA collisions,” *Phys. Rev.* **C75** (2007) 034908, [arXiv:hep-ph/0606236](#).
- [33] I. Lokhtin and A. Snigirev, “A Model of jet quenching in ultrarelativistic heavy ion collisions and high-p(T) hadron spectra at RHIC,” *Eur.Phys.J.* **C45** (2006) 211–217, [arXiv:hep-ph/0506189 \[hep-ph\]](#).
- [34] K. Zapp, J. Stachel, and U. A. Wiedemann, “A Local Monte Carlo implementation of the non-abelian Landau-Pomeranchuk-Migdal effect,” *Phys.Rev.Lett.* **103** (2009) 152302, [arXiv:0812.3888 \[hep-ph\]](#).
- [35] N. Armesto, L. Cunqueiro, and C. A. Salgado, “Q-PYTHIA - a Monte Carlo implementation for jet quenching,” [arXiv:0906.0754 \[hep-ph\]](#).
- [36] N. Armesto, G. Corcella, L. Cunqueiro, and C. A. Salgado, “Angular-ordered parton showers with medium-modified splitting functions,” *JHEP* **0911** (2009) 122, [arXiv:0909.5118 \[hep-ph\]](#).
- [37] B. Schenke, C. Gale, and S. Jeon, “MARTINI: An Event generator for relativistic heavy-ion collisions,” *Phys.Rev.* **C80** (2009) 054913, [arXiv:0909.2037 \[hep-ph\]](#).
- [38] T. Renk, “YaJEM: a Monte Carlo code for in-medium shower evolution,” [arXiv:1009.3740 \[hep-ph\]](#).
- [39] A. Leonidov and V. Nechitailo, “Decoherence and energy loss in QCD cascades in nuclear collisions,” *Eur. Phys. J.* **C71** (2011) 1537, [arXiv:1006.0366 \[nucl-th\]](#).